# Self-similar interpolation in quantum mechanics

V. I. Yukalov,[1,2] E. P. Yukalova,[1,2] and S. Gluzman[3]
[1]*Centre for Interdisciplinary Studies in Chemical Physics, University of Western Ontario, London, Ontario, Canada N6A 3K7*
[2]*Bogolubov Laboratory of Theoretical Physics, Joint Institute for Nuclear Research, Dubna, Russia*
[3]*International Centre of Condensed Matter Physics, University of Brasilia, Caixa Postal 04513, Brasilia, Distrito Federal 70919–970, Brazil*
(Received 7 November 1997)

An approach is developed for constructing simple analytical formulas accurately approximating solutions to eigenvalue problems of quantum mechanics. This approach is based on self-similar approximation theory. In order to derive interpolation formulas valid in the whole range of parameters of considered physical quantities, the self-similar renormalization procedure is complemented here by boundary conditions which define control functions guaranteeing correct asymptotic behavior in the vicinity of boundary points. To emphasize the generality of the approach, it is illustrated by different problems that are typical for quantum mechanics, such as anharmonic oscillators, double-well potentials, and quasiresonance models with quasistationary states. In addition, the nonlinear Schrödinger equation is considered, for which both eigenvalues and wave functions are constructed. [S1050-2947(98)03207-7]

PACS number(s): 03.65.Ge, 02.30.Lt, 02.30.Mv

## I. INTRODUCTION

A standard problem in quantum mechanics is how to solve approximately stationary Schrödinger equations that do not possess exact solutions. In the cases of asymptotically small and asymptotically large coupling parameters, one may employ perturbation theory presenting solutions as power series in powers of the corresponding small parameter. However, such series are practically always only asymptotic and quickly diverge for sufficiently small expansion parameters. Moreover, physical quantities of interest usually correspond neither to weak-coupling nor to strong-coupling limits, but to an intermediate region of a coupling parameter. Thus the problem arises of how to construct an interpolation formula, valid in the whole region of physical variables, when only asymptotic expansions near boundaries are known.

The most known method of deriving interpolation formulas is the two-point Padé approximation [1–3]. In some cases the latter yields quite reasonable results. Nevertheless, the usage of this method has not become widespread because of the following difficulties.

First of all, to reach sufficient accuracy by employing Padé approximants, one needs to have tens of terms in perturbative expansions [1–3]. But the standard situation in physically interesting problems is when one has in hand only a few terms. In such a case, for the same problem one may construct different two-point Padé approximants, all having correct left-side and right-side limits, but differing from each other in the intermediate region by 1000% [4]. This clearly shows that in the case of short series the two-point Padé approximants cannot provide even qualitative description.

Second, two-point Padé approximants can treat at infinity only rational powers [1–3] and are not able to describe other types of behavior, for example, power laws with irrational powers or exponential functions. However, behavior that is more complicated than the rational-power behavior often occurs in physical problems. For instance, exponential behavior at infinity is constantly exhibited by wave functions.

Third, interpolation between two different expansions, by using two-point Padé approximants, can be accomplished solely when these two expansions have compatible variables [1–3]. For example, even for such a simple problem as the anharmonic oscillator, the eigenvalues in the weak-coupling and strong-coupling expansions have incompatible variables [5].

Fourth, there exists the well-known and annoying problem of appearance of poles in Padé approximants, which results in unphysical singularities [1–3]. Eliminating such singularities in two-point Padé approximants is often impossible because of restrictions that are imposed by prescribed boundary conditions.

Finally, Padé approximation is rather a numerical technique, but we keep in mind an *analytical* approach that would combine relatively simple representation for physical quantities with their good accuracy. The advantage of having analytical expressions, as compared to just numbers obtained from a numerical procedure, is in the convenience of analyzing such expressions with respect to physical parameters entering into them.

In the present paper we develop an analytical approach for deriving interpolation formulas, which is free of the above deficiencies of Padé approximation. This approach works well when just a few terms of asymptotic expansions are available; it successfully sews power-law with exponential asymptotic behavior; it does not have at all the problem of compatibility; no unphysical poles arise; it combines analytical representation with good accuracy. We illustrate the approach by several quantum-mechanical problems that are usually considered as typical touchstones for any new method. These problems include calculation of energy levels for different anharmonic oscillators, for the Hamiltonians with double-well potentials, and for quasiresonance models. Each of these problems has its own specific calculational difficulties (for review see Refs. [5–7]). This is why it is important to show that all of them can be treated by the same approach. Moreover, we demonstrate that the same method

 

is applicable to the *nonlinear* Schrödinger equation, for which we find both the energy and wave function of the ground state. The latter example is interesting not only as an illustration of wide possibilities of the approach, but it is important for practical purposes, being related to the description of Bose-condensed particles in traps. We carefully compare the properties of the wave function we have derived with those of the Thomas-Fermi and variational-Gaussian approximations. The analysis proves that our wave function provides the best approximation for a solution to the nonlinear Schrödinger equation considered. Analytical expressions for the wave function of a vertex filament are also constructed, being in good agreement with numerical data.

## II. SELF-SIMILAR INTERPOLATION

Assume that we are interested in finding a function $f(x)$ in the interval $x_1 \leqslant x \leqslant x_2$. The latter can be finite or infinite. Let equations defining the function $f(x)$ be rigorously unsolvable, so that only perturbative asymptotic expansions near the boundaries can be derived: near the left boundary,

$$f(x) \simeq p_k(x,x_1), \quad x \rightarrow x_1 + 0 \tag{1}$$

and near the right boundary,

$$f(x) \simeq p_k(x,x_2), \quad x \rightarrow x_2 - 0 \tag{2}$$

where $k = 0,1,2, \ldots$ . For the time being, we do not specify the physical nature of the function $f(x)$ and its variable $x$, since the general scheme does not depend on these specifications.

In this section we develop such a general scheme for constructing approximations to the function $f(x)$, so that these approximations, interpolating between the asymptotic expansions (1) and (2), could be valid in the whole region $x_1 \leqslant x \leqslant x_2$. The approach we develop is based on the self-similar approximation theory [8–13] in its algebraically invariant formulation [14–16]. Here we show how to construct self-similar approximations so that they be compatible with the asymptotic boundary conditions (1) and (2). Since all theoretical foundation and basic technical details of the method have been expounded in our previous papers [8–16], we do not repeat them here but only delineate the scheme of the approach adapting it to the considered problem of interpolation.

Let us take an asymptotic expansion, like Eq. (1) or Eq. (2), in the vicinity of a point $x_i$, with $i = 1,2$. Define the algebraic transform

$$P_k(x,s,x_i) = x^s p_k(x,x_i), \tag{3}$$

whose inverse, evidently, is

$$p_k(x,x_i) = x^{-s} P_k(x,s,x_i). \tag{4}$$

Introduce an expansion function $x(\varphi,s,x_i)$ by means of the equation

$$P_0(x,s,x_i) = \varphi, \quad x = x(\varphi,s,x_i). \tag{5}$$

Substituting this expansion function into Eq. (3), we obtain

$$y_k(\varphi,s,x_i) = P_k(x(\varphi,s,x_i),s,x_i). \tag{6}$$

Transformation inverse to Eq. (6) reads

$$P_k(x,s,x_i) = y_k(P_0(x,s,x_i),s,x_i). \tag{7}$$

The family $\{y_k\}$ of the endomorphisms defined in Eq. (6) is called [11–13] the approximation cascade, because its trajectory $\{y_k(\varphi,s,x_i)\}$ is bijective to the sequence of approximations $\{P_k(x,s,x_i)\}$. The cascade velocity can be given by the finite difference

$$v_k(\varphi,s,x_i) = y_k(\varphi,s,x_i) - y_{k-1}(\varphi,s,x_i). \tag{8}$$

The evolution equation, written in the integral form, is

$$\int_{P_{k-1}}^{P_k^*} \frac{d\varphi}{v_k(\varphi,s,x_i)} = \tau, \tag{9}$$

where $P_k = P_k(x,s,x_i)$, the upper limit $P_k^* = P_k^*(x,s,\tau,x_i)$ is a self-similar approximation corresponding to a quasifixed point, and $\tau$ is an effective time necessary for reaching this quasifixed point. The latter, in accordance with the inverse algebraic transform (4), yields

$$p_k^*(x,s,\tau,x_i) = x^{-s} P_k^*(x,s,\tau,x_i). \tag{10}$$

To illustrate these steps, consider an asymptotic expansion

$$p_k(x,0) = \sum_{n=0}^{k} a_n x^n \tag{11}$$

in the vicinity of $x_1 = 0$. Then, accomplishing the described procedure, for Eq. (10) we find

$$p_k^*(x,s,\tau,0) = \left[ p_{k-1}^{-k/s}(x,0) - \frac{k a_k \tau}{s a_0^{1+k/s}} x^k \right]^{-s/k}. \tag{12}$$

An important particular case is when $s \rightarrow \infty$, then Eq. (12) gives

$$\lim_{s\rightarrow\infty} p_k^*(x,s,\tau,0) = p_{k-1}(x,0) \exp\left( \frac{a_k}{a_0} \tau x^k \right). \tag{13}$$

This shows how exponential functions naturally appear in our method, together with the radical expressions of type (12).

An expression $p_k^*$, given either by Eq. (12) or by Eq. (13), as is seen, is a function of a lower-order series $p_{k-1}$,

$$p_k^* = F_k(p_{k-1}). \tag{14}$$

Analogously to the way by which we have come from an asymptotic series $p_k$ to the renormalized expression $p_k^*$, we can renormalize $p_{k-1}$ entering into relation (14), which gives

$$p_k^{**} = F_k(p_{k-1}^*) = F_k(F_{k-1}(p_{k-2})). \tag{15}$$

Repeating such a renormalization $k$ times, we come to

$$p_k^{*\cdots*} = F_k(F_{k-1}(\cdots F_1(p_0))\cdots). \tag{16}$$

At each $n$ step of renormalization (14), two parameters, $s_n$ and $\tau_n$, arise in the resulting expression, according to Eq. (12). Therefore the $k$-times renormalized quantity (16) contains $2k$ such parameters,

$$p_k^{*\cdots *} \equiv F_k^*(x,\overline{s}_k,\overline{\tau}_k,x_i), \tag{17}$$

where the shorthand notation

$$\overline{s}_k \equiv \{s_1,s_2,\ldots,s_k\}, \quad \overline{\tau}_k \equiv \{\tau_1,\tau_2,\ldots,\tau_k\}$$

is used.

The sets $\overline{s}_k$ and $\overline{\tau}_k$ are to be defined so that the renormalization procedure would converge to a function satisfying the boundary conditions (1) and (2). Suppose that we started from a series $p_k(x,x_i)$ written for an asymptotic region of $x_i$, with $i=1,2$. Renormalizing this series $2k$ times, we get Eq. (17). In order that the renormalized expression (17) could satisfy the correct asymptotic behavior at another boundary point $x_j$, with $j\neq i$, we have to require the asymptotic condition

$$F_k^*(x,\overline{s}_k,\overline{\tau}_k,x_i) \rightarrow p_k(x,x_j), \quad x\rightarrow x_j. \tag{18}$$

Condition (18) defines the control sets

$$\overline{s}_k = \overline{s}_k(x), \quad \overline{\tau}_k = \overline{\tau}_k(x) \tag{19}$$

of control functions $s_1(x),s_2(x),\ldots,s_k(x)$, and $\tau_1(x),\tau_2(x),\ldots,\tau_k(x)$. Substituting these control functions into Eq. (17), we obtain the final self-similar approximant

$$f_k^*(x,x_i) = F_k^*(x,\overline{s}_k(x),\overline{\tau}_k(x),x_i). \tag{20}$$

Control functions are called so because of their role of controlling convergence of the procedure to a function having the desired properties [17]. In general, these functions are, really, functions of $x$, although in particular cases they can become just parameters. In the latter case, they can be called control parameters.

In order to make the above procedure transparent, let us consider a typical case of two asymptotic expansions at $x_1=0$ and $x_2=\infty$. Assume that at the left boundary we have a sequence

$$p_1(x,0)=a_0+a_1x, \quad p_2(x,0)=a_0+a_1x+a_2x^2,\ldots \tag{21}$$

of perturbative expansions $p_k(x,0)$, and at the right boundary, a sequence

$$p_1(x,\infty)=Ax^n, \quad p_2(x,\infty)=Ax^n+Bx^m,\ldots \tag{22}$$

of asymptotic expressions $p_k(x,\infty)$, with $n\geqslant m$. Starting from $p_1(x,0)$, according to Eq. (12), we get

$$p_1^*(x,s,\tau,0)=\left(a_0^{-1/s}-\frac{a_1\tau}{sa_0^{1+1/s}}x\right)^{-s}. \tag{23}$$

As the asymptotic boundary condition (18), we have

$$p_1^*(x,s,\tau,0)\rightarrow p_1(x,\infty), \quad x\rightarrow\infty \tag{24}$$

with $p_1(x,\infty)$ given by Eq. (22). Condition (24) holds true if and only if

$$s=-n, \quad \tau = n\frac{a_0}{a_1}\left(\frac{A}{a_0}\right)^{1/n}. \tag{25}$$

Therefore the first-order self-similar approximant, defined by Eq. (20), becomes

$$f_1^*(x,0)=(a_0^{1/n}+A^{1/n}x)^n. \tag{26}$$

Similarly, starting from $p_2(x,0)$ given in Eq. (21), we find the twice renormalized expression

$$F_2^*(x,s_1,\tau_1,s_2,\tau_2,0) = \left\{[p_1^*(x,s_1,\tau_1,0)]^{-2/s_2}-\frac{2a_2\tau_2}{s_2a_0^{1+2/s_2}}x^2\right\}^{-s_2/2}. \tag{27}$$

Imposing the asymptotic boundary condition

$$F_2^*(x,s_1,\tau_1,s_2,\tau_2,0)\rightarrow p_1(x,\infty), \quad x\rightarrow\infty \tag{28}$$

we obtain

$$s_2=-n, \quad \tau_2=\frac{na_0}{2a_2}\left(\frac{A}{a_0}\right)^{2/n}. \tag{29}$$

Employing Eq. (29) for Eq. (27), we have

$$F_2^*(x,s_1,\tau_1,s_2,\tau_2,0)=\{[p_1^*(x,s_1,\tau_1,0)]^{2/n}+A^{2/n}x^2\}^{n/2}. \tag{30}$$

The boundary condition

$$F_2^*(x,s_1,\tau_1,s_2,\tau_2,0)\rightarrow p_2(x,\infty), \quad x\rightarrow\infty \tag{31}$$

is satisfied provided that

$$s_1=-\frac{n}{2}q, \quad \tau_1=-s_1\frac{a_0}{a_1}\left(\frac{A}{a_0}\right)^{2/nq}\left(\frac{2B}{nA}\right)^{1/q}, \tag{32}$$

where the notation

$$q\equiv 2+m-n<2 \quad (n>m) \tag{33}$$

is used. With the control parameters given by Eq. (32), the function $p_1^*$ entering into Eq. (30) writes

$$p_1^*(x,s_1,\tau_1,0)=\left[a_0^{2/nq}+A^{2/nq}\left(\frac{2B}{nA}\right)^{1/q}x\right]^{nq/2}. \tag{34}$$

Combining Eq. (30) with Eq. (34), we obtain the second-order self-similar approximant

$$f_2^*(x,0)=\left\{\left[a_0^{2/nq}+A^{2/nq}\left(\frac{2B}{nA}\right)^{1/q}x\right]^q+A^{2/n}x^2\right\}^{n/2}, \tag{35}$$

defined in Eq. (20). In the same way, we may proceed farther calculating a $k$-order self-similar approximant.

To complete this calculational procedure, we need to answer the following question. Assume that we have two asymptotic expansions near two boundary points. We may start from one of these expansions, say $p_k(x,x_1)$, imposing

the boundary condition, as in Eq. (18), at another boundary point, in this case at $x_2$, and thus obtaining the self-similar approximant $f_k^*(x,x_1)$. The same procedure could be accomplished, starting from $p_k(x,x_2)$ and imposing the boundary condition at $x_1$, thus getting $f_k^*(x,x_2)$. The question that arises is which of these two approximants, $f_k^*(x,x_1)$ or $f_k^*(x,x_2)$, is expected to be more accurate?

The answer to this question can be done from the point of view of stability analysis [11–13]. To this end, let us take an expansion $p_k(x,x_i)$ near a point $x_i$, with $i=1,2$. Suppose that $p_0(x,x_i)$ depends on $x$. If $p_0(x,x_i)$ does not depend on $x$, we have to take $p_1(x,x_i)$. Define the expansion function $x(\varphi,x_i)$ by the equation

$$p_0(x,x_i)=\varphi, \quad x=x(\varphi,x_i). \tag{36}$$

Introduce

$$y_k(\varphi,x_i)=p_k(x(\varphi,x_i),x_i), \tag{37}$$

being a trajectory point of an approximation cascade $\{y_k^i\}$ formed by the family of endomorphisms from Eq. (37). The stability of the cascade trajectory is characterized by the local multipliers

$$\mu_k(\varphi,x_i)\equiv\frac{\partial}{\partial\varphi}y(\varphi,x_i), \tag{38}$$

whose images in the $x$ space are given by the local multipliers

$$m_k(x,x_i)\equiv\mu_k(p_0(x,x_i),x_i)=\frac{\delta p_k(x,x_i)}{\delta p_0(x,x_i)}=\frac{\partial p_k(x,x_i)/\partial x}{\partial p_0(x,x_i)/\partial x}. \tag{39}$$

The smaller absolute values $|m_k(x,x_i)|$ of the multipliers correspond to the more stable trajectory of the associated cascade, and the higher stability implies the better convergence property of the related sequence of approximations [12,13]. Therefore, in the asymptotic boundary condition (18), we must choose that asymptotic expansion $p_k(x,x_j)$ which corresponds to the more stable cascade trajectory.

If two multipliers, $m_k(x,x_1)$ and $m_k(x,x_2)$, are equal or close to each other, then we cannot decide *a priori* which of the self-similar approximants, $f_k^*(x,x_1)$ or $f_k^*(x,x_2)$, is preferable. In such a case, it is logical to define the average self-similar approximation

$$f_k^*(x)\equiv\frac{1}{2}[f_k^*(x,x_1)+f_k^*(x,x_2)]. \tag{40}$$

Usually, one of the approximations $f_k^*(x,x_i)$, where $i=1,2$, lies below, and another above the exact function $f(x)$. In such a case, the errors of these approximants compensate each other, essentially improving the accuracy of the average approximant (40).

## III. ANHARMONIC OSCILLATORS

We start illustrating our interpolation approach with the models of one-dimensional anharmonic oscillators described by the Hamiltonian

$$H=-\frac{1}{2}\frac{d^2}{dx^2}+\frac{1}{2}x^2+gx^m, \tag{41}$$

in which the space variable $x\in(-\infty,+\infty)$, the coupling parameter $g\in[0,\infty)$, and the power $m\geqslant 4$. These models are classical touchstones from which everyone starts considering a new method.

Let us be interested in finding the ground-state energy $e(g)$ as a function of the coupling parameter $g$. For this function, the asymptotic expansions in the weak- and strong-coupling limits are known. In the weak-coupling limit, perturbation theory gives

$$e_k(g,0)=\sum_{n=0}^{k} a_n g^n \quad (g\to 0). \tag{42}$$

This series strongly diverges for any $g\neq 0$, since the coefficients $a_n$ grow like $n!$ as $n\to\infty$ [18,19]. The coefficients $a_n$ are, of course, different for different types of oscillators, depending on $m$. However, for the sake of simplicity, we do not use the double indexing. In the strong-coupling limit, one has [20] the expansion

$$e_k(g,\infty)=\sum_{n=0}^{k} A_n g^{2(1-2n)/(m+2)} \quad (g\to\infty). \tag{43}$$

Here again the coefficients $A_n$ depend on $m$, that is, on the kind of oscillator. Not marking this dependence explicitly will not lead to confusion, since different kinds of oscillators will be considered separately.

### A. Quartic oscillator

Start with the quartic oscillator with $m=4$. For the first several coefficients of the weak-coupling series (42), one has [18,19]

$$a_0=\frac{1}{2}, \quad a_1=\frac{3}{4}, \quad a_2=-\frac{21}{8}, \quad a_3=\frac{333}{16}, \ldots .$$

The coefficients of the strong-coupling expansion (43) have been computed by many authors, starting from Hioe and Montroll [21]. One of the most accurate computations have been accomplished by Weniger [22]. The values of the strong-coupling coefficients are $A_0=0.667\,986$, $A_1=0.143\,669$, $A_2=-0.008\,628$, $A_3=0.000\,818$, $A_4=-0.000\,082$, $A_5=0.000\,008$.

Following the approach described in Sec. II, we may start from the weak-coupling series (42) and define control functions from the asymptotic condition (18) with $e_k(g,\infty)$ given by the strong-coupling expansion (43). In the second order this gives

$$e_2^*(g,0)=\left[a_0^6\left(1+\frac{9a_1}{2a_0}\tau_0 g\right)^{4/3}+A_0^6 g^2\right]^{1/6},$$

with the control parameter

$$\tau_0=\frac{4A_0^4A_1}{3a_0^4a_1}\left(\frac{a_0^2}{6A_0A_1}\right)^{1/4}=0.660\,46.$$

As a result, we obtain

$$e_2^*(g,0)=[a_0^6(1+Cg)^{4/3}+A_0^6g^2]^{1/6}, \tag{44}$$

where

$$C=\frac{6A_0^4A_1}{a_0^5}\left(\frac{a_0^2}{6A_0A_1}\right)^{1/4}.$$

In the same way, starting from the strong-coupling expansion (43) and defining control functions from asymptotic condition (18) at the left boundary, we find

$$e_2^*(g,\infty)=[a_0^4+(16a_0^6a_1^2+A_0^8g^{2/3})^{1/2}g]^{1/4}. \tag{45}$$

Numerical calculations show that both approximants (44) and (45) are close to each other. The accuracy of a self-similar approximant $e_k^*(g,x_i)$ can be estimated by comparing the values it gives for different coupling parameters $g$, with precise numerical calculations accomplished by Hioe and Montroll [21] for $g$ in the interval $0.02\leqslant g\leqslant 20\,000$. The maximal percentage error of the left approximant (44) is $-2.9\%$ occurring at $g=0.3$, and the largest error of Eq. (45) is 4.2% at $g=2$. For all $g$, the left approximant (44) lies below the exact values of the energy, while the right approximant (45) is above the exact values. The average self-similar approximant

$$e_2^*(g)=\frac{1}{2}[e_2^*(g,0)+e_2^*(g,\infty)]$$

has the maximal error of 1.4% at $g=2$.

As we see, a quite simple analytical expression provides sufficiently good accuracy, with the maximal error around 1%. As far as the structure of perturbative series for the quartic anharmonic oscillator is analogous to that of series for the so-called $\varphi^4$ model of quantum field theory [23], we may hope that for the latter one also could construct analogous self-similar approximants.

### B. Sextic oscillator

The sextic oscillator ($m=6$) is interesting being a borderline case between the models whose perturbative series are Padé summable and those whose series cannot be summed. For the sextic oscillator, Padé approximants converge so slowly that they are computationally useless [5,24].

Employing the approach of Sec. II, we use the coefficients $A_0=0.680\,703$, $A_1=0.129\,464$, $A_2=-0.005\,512$, $A_3=0.000\,328$, $A_4=-0.000\,018$, $A_5=0.000\,001$. We find the first self-similar approximants, from the left,

$$e_1^*(g,0)=\frac{1}{2}(1+16A_0^4g)^{1/4}, \tag{46}$$

and from the right,

$$e_1^*(g,\infty)=\frac{1}{2}(1+4A_0^2g^{1/2})^{1/2}. \tag{47}$$

The maximal error of Eq. (46), with respect to accurate numerical results [5] that can be treated as exact, is about $-11\%$, and the maximal error of Eq. (47) is about 8%.

In the second order, we find

$$e_2^*(g,0)=\frac{1}{2}[(1+2Cg)^{3/2}+(2A_0)^8g^2]^{1/8}, \tag{48}$$

where $C=3.428$, with the maximal error $-6\%$. The right approximant has a comparable accuracy.

The third-order left approximant is

$$e_3^*(g,0)=\frac{1}{2}\{[(1+2B_1g)^{3/2}+4B_2g^2]^{5/4}+(2A_0)^{12}g^3\}^{1/12}, \tag{49}$$

where $B_1=4.831$ and $B_2=9.352$. The maximal error is around $-4\%$.

The fourth-order approximant can be written as

$$e_4^*(g,0)=\frac{1}{2}(\{[(1+2C_1g)^{3/2}+4C_2g^2]^{5/4}+8C_3g^3\}^{7/6}+(2A_0)^{16}g^4)^{1/16}, \tag{50}$$

with $C_1=6.078$, $C_2=18.143$, and $C_3=22.322$. The maximal error is about $-3\%$.

In the fifth order, we find

$$e_5^*(g,0)=\frac{1}{2}[(\{[(1+2D_1g)^{3/2}+4D_2g^2]^{5/4}+8D_3g^3\}^{7/6}+16D_4g^4)^{9/8}+(2A_0)^{20}g^5]^{1/20}, \tag{51}$$

where $D_1=7.215$, $D_2=28.848$, $D_3=56.001$, and $D_4=49.39$. The maximal error is $-2.5\%$.

For the sixth order, we obtain

$$e_6^*(g,0)=\frac{1}{2}\{[(\{[(1+2K_1g)^{3/2}+4K_2g^2]^{5/4}+8K_3g^3\}^{7/6}+16K_4g^4)^{9/8}+32K_5g^5]^{11/10}+(2A_0)^{24}g^6\}^{1/24}, \tag{52}$$

with the coefficients $K_1=8.256$, $K_2=41.122$, $K_3=109.122$, $K_4=153.119$, and $K_5=104.156$. The maximal error of approximant (52) is $-2\%$.

Equations (46)–(52) show that the accuracy of the self-similar approximants improves with increasing order. To demonstrate that there is uniform numerical convergence for all $g$, we present in Table I the percentage errors $\varepsilon_k^*(g,x_i)$ of the corresponding approximants $e_k^*(g,x_i)$, as compared to exact values $e(g)$. The accuracy in each order can also be improved by defining the average approximants (40). We show this for the case of the approximant

$$e_1^*(g)=\frac{1}{2}[e_1^*(g,0)+e_1^*(g,\infty)], \tag{53}$$

whose errors are also presented in Table I.

TABLE I. Percentage errors of the self-similar approximants for the ground-state energy of the sextic oscillator, as compared to numerical data for $e(g)$.

| $g$ | $e(g)$ | $\varepsilon_1^*(g,0)$ | $\varepsilon_1^*(g,\infty)$ | $\varepsilon_1^*(g)$ | $\varepsilon_2^*(g,0)$ | $\varepsilon_3^*(g,0)$ | $\varepsilon_4^*(g,0)$ | $\varepsilon_5^*(g,0)$ | $\varepsilon_6^*(g,0)$ |
|---|---|---|---|---|---|---|---|---|---|
| 0.1 | 0.586945 | −8.25 | 7.25 | −0.50 | −5.45 | −3.99 | −3.06 | − 2.46 | −1.95 |
| 0.5 | 0.717813 | −10.56 | 5.88 | −2.34 | −4.71 | −2.48 | −1.44 | − 0.88 | −0.53 |
| 2 | 0.915219 | −8.47 | 3.99 | −2.24 | −2.40 | −0.82 | −0.33 | − 0.11 | −0.06 |
| 50 | 1.858487 | −2.47 | 1.03 | −0.67 | −0.16 | −0.03 | 0 | 0 | 0 |
| 1000 | 3.850896 | −0.59 | 0.25 | −0.16 | −0.01 | 0 | 0 | 0 | 0 |

### C. Octic oscillator

The case of the octic oscillator ($m=8$) is important to consider remembering that Padé approximants are not able to sum the corresponding perturbation series [24,25]. As we show below, in our approach we obtain a series of self-similar approximants exhibiting uniform numerical convergence.

Here we use the following coefficients $A_0=0.704\,046$, $A_1=0.120\,626$, $A_2=-0.004\,168$, $A_3=0.000\,188$, $A_4=-0.000\,007$, $A_5=0.000\,001$. The first-order left approximant reads

$$e_1^*(g,0)=\frac{1}{2}(1+32A_0^5g)^{1/5}, \tag{54}$$

while the right approximant is

$$e_1^*(g,\infty)=\frac{1}{2}(1+4A_0^2g^{2/5})^{1/2}. \tag{55}$$

Comparing this with numerical results [5], we find that the maximal error of Eq. (54) is about $-13\%$ and that of Eq. (55) is $8\%$.

For the second-order left approximant we have

$$e_2^*(g,0)=\frac{1}{2}[(1+2Cg)^{8/5}+(2A_0)^{10}g^2]^{1/10}, \tag{56}$$

with $C=5.944$, the maximal error being $-8\%$.

In the third order, we get

$$e_3^*(g,0)=\frac{1}{2}\{[(1+2B_1g)^{8/5}+4B_2g^2]^{13/10}+(2A_0)^{15}g^3\}^{1/5}, \tag{57}$$

where $B_1=8.671$ and $B_2=26.807$. The maximal error is $-6\%$.

The fourth-order approximant is

$$e_4^*(g,0)=\frac{1}{2}(\{[(1+2C_1g)^{8/5}+4C_2g^2]^{13/10}+8C_3g^3\}^{6/5}+(2A_0)^{20}g^4)^{1/20}, \tag{58}$$

with $C_1=11.151$, $C_2=55.077$, and $C_3=104.667$. The maximal error is $-4.5\%$.

The fifth-order approximant writes

$$e_5^*(g,0)=\frac{1}{2}[(\{[(1+2D_1g)^{8/5}+4D_2g^2]^{13/10}+8D_3g^3\}^{6/5}+16D_4g^4)^{23/20}+(2A_0)^{25}g^5]^{1/25}, \tag{59}$$

where $D_1=13.443$, $D_2=91.126$, $D_3=282.775$, and $D_4=377.013$. The maximal error is $-3.5\%$.

For the sixth order, we obtain

$$e_6^*(g,0)=\frac{1}{2}\{[(\{[(1+2K_1g)^{8/5}+4K_2g^2]^{13/10}+8K_3g^3\}^{6/5}+16K_4g^4)^{23/20}+32K_5g^5]^{28/25}+(2A_0)^{30}g^6\}^{1/30}, \tag{60}$$

where $K_1=15.508$, $K_2=133.486$, $K_3=581.021$, $K_4=1274$, and $K_5=1291$. The maximal error is $-3\%$.

As we see, in our approach there is no principal difference between the types of oscillators, whether it is quartic, sextic, or octic; for each of them we can easily construct a uniformly convergent sequence of self-similar approximants. The accuracy of the latter in each order can be essentially improved by composing average approximants, as in Eq. (53). The errors of the obtained approximants are collected in Table II.

Let us emphasize that our aim here was to derive *analytical* formulas. The approximants we have constructed are easier to use than more complicated expressions that follow from renormalized perturbation theory [17], in which control functions are introduced into a zero-order Hamiltonian

TABLE II. Percentage errors of the self-similar approximants for the ground-state energy of the octic oscillator.

| $g$ | $e(g)$ | $\varepsilon_1^*(g,0)$ | $\varepsilon_1^*(g,\infty)$ | $\varepsilon_1^*(g)$ | $\varepsilon_2^*(g,0)$ | $\varepsilon_3^*(g,0)$ | $\varepsilon_4^*(g,0)$ | $\varepsilon_5^*(g,0)$ | $\varepsilon_6^*(g,0)$ |
|---|---|---|---|---|---|---|---|---|---|
| 0.1 | 0.620514 | −12.01 | 7.82 | −2.10 | −7.90 | −5.72 | −4.27 | −3.30 | −2.66 |
| 0.5 | 0.745510 | −12.54 | 6.10 | −3.22 | −5.77 | −3.15 | −1.88 | −1.21 | −0.81 |
| 2 | 0.911090 | −9.66 | 4.39 | −2.64 | −3.13 | −1.26 | −0.60 | −0.27 | −0.17 |
| 50 | 1.594327 | −3.38 | 1.52 | −0.93 | −0.43 | −0.08 | −0.02 | 0 | 0 |
| 1000 | 2.833102 | −1.06 | 0.49 | −0.28 | −0.04 | 0 | 0 | 0 | 0 |

[6,7,26–31]. This especially concerns the sextic and octic oscillators. We think that the possibility to have simple and accurate formulas, valid for the whole range of coupling parameters, is an advantage of our approach that could be a useful tool for analyzing the properties of quantum dots [32–34].

## IV. DOUBLE-WELL OSCILLATORS

Models with double-well potentials are notoriously known to be difficult for approximate treatment. For instance, perturbation theory in this case results in series that are not Padé summable. At the same time such potentials are quite common for various problems encountered in physics and chemistry (see discussion in Ref. [35]).

One of the difficulties of dealing with double-well models is that the corresponding physical quantities, as functions of the coupling parameter, can display not two characteristic regions of behavior, that is, the weak-coupling and the strong-coupling regions, but a third region, intermediate between weak and strong coupling. This behavior is similar to that of some models of quantum field theory where in the transition region instanton effects are crucial, bridging the weak- and strong-coupling limits [36,37].

### A. Zero-dimensional model

Let us, first, consider the so-called zero-dimensional double-well model whose free energy is written as

$$f(g)=-\ln Z(g), \tag{61}$$

where

$$Z(g)=\frac{1}{\sqrt{\pi}}\int_{-\infty}^{+\infty}\exp\{-H(x)\}dx \tag{62}$$

plays the role of a partition function with the Hamiltonian

$$H(x)=-x^2+gx^4, \quad g\geqslant 0. \tag{63}$$

The latter has a maximum $H(0)=0$ at $x=0$ and two minima $H(\pm a)=-1/4g$ at $x=\pm a=\pm 1/\sqrt{2g}$.

Direct use of perturbation theory, in powers of $g$, to the free energy (61) is impossible, since $f(g)\to-\infty$ as $g\to 0$. Thence, a special procedure is necessary. To this end, we define the trial Hamiltonians

$$H_{\pm}(x)=\omega^2(x\pm a)^2-u_0, \tag{64}$$

in which

$$a=\frac{1}{\sqrt{2g}}, \quad u_0=\frac{1}{4g},$$

and $\omega$ is a trial parameter to become later a control function. The partition function (62) can be written in the form

$$Z(g)=\frac{1}{2\sqrt{\pi}}\int_{-\infty}^{+\infty}\exp\{-H_+(x)-\Delta H_+(x)\}dx + \frac{1}{2\sqrt{\pi}}\int_{-\infty}^{+\infty}\exp\{-H_-(x)-\Delta H_-(x)\}dx, \tag{65}$$

where

$$\Delta H_{\pm}=H(x)-H_{\pm}(x).$$

The free energy (61) is expanded in powers of $\Delta H_{\pm}(x)$, with the zero-order term

$$F_0(g,\omega)=\ln\omega-u_0, \tag{66}$$

the first-order term

$$F_1(g,\omega)=\ln\omega-a^2-\frac{1}{2\omega^2}-\frac{1}{2}+\left(a^4+\frac{3a^2}{\omega^2}+\frac{3}{4\omega^4}\right)g, \tag{67}$$

and so on.

The control function $\omega(g)$ is defined from the quasifixed-point condition

$$\frac{\partial}{\partial\omega}F_1(g,\omega)=0, \tag{68}$$

which gives

$$\omega(g)=\left(\frac{3g}{\sqrt{1+3g}-1}\right)^{1/2}. \tag{69}$$

This control function in the weak-coupling limit, as $g\to 0$, behaves as

$$\omega(g)\simeq\sqrt{2}\left(1+\frac{3}{8}g-\frac{45}{128}g^2\right), \tag{70}$$

and in the strong-coupling limit, as $g\to\infty$, it has the asymptotic behavior

$$\omega(g)\simeq(3g)^{1/4}+\frac{1}{2}(3g)^{-1/4}+\frac{1}{8}(3g)^{-3/4}. \tag{71}$$

For $g\in[0,\infty)$, function (69) changes in the interval $\sqrt{2}\leqslant\omega(g)<\infty$.

Defining

$$f_k(g)\equiv F_k(g,\omega(g)), \tag{72}$$

from Eqs. (66) and (67) we have

$$f_0(g)=\ln\omega-\frac{1}{4g}, \quad f_1(g)=\ln\omega-\frac{1}{4g}-\frac{1}{4}+\frac{1}{2\omega^2}. \tag{73}$$

Similarly, calculating $F_2(g,\omega)$, we come in the second order to

$$f_2(g)=\ln\omega-\frac{1}{4g}-\frac{1}{3}-\frac{5}{3\omega^2}+\frac{14}{3\omega^4}. \tag{74}$$

Wishing to estimate the accuracy of the approximations $f_1(g)$ and $f_2(g)$, let us notice that the exact function (61) changes from $-\infty$ as $g\to 0$ to $+\infty$ as $g\to\infty$, crossing zero at $g=g_c=2.758$, that is, $f(g_c)=0$. Therefore we cannot define the percentage error in the standard way as $100\%\times[f_k(g)-f(g)]/f(g)$, since such a definition contains zero in the denominator. Instead of this, we may evaluate the accuracy of a crossing point given by the corresponding approximation, that is, the accuracy of the solution $g_c^{(k)}$ to the equation

$$f_k(g_c^{(k)})=0. \tag{75}$$

For the first approximation, we have $g_c^{(1)}=0.585$ which gives the error of $-79\%$, as compared to the exact $g_c=2.758$. For the second approximation, we get $g_c^{(2)}=1.352$, whose error is $-51\%$. As is seen, this accuracy is not high, so that it is desirable to improve it.

Introduce the function

$$\alpha(g)\equiv\frac{1}{\omega^2(g)}=\frac{\sqrt{1+3g}-1}{3g}. \tag{76}$$

This function changes in the interval $0\leqslant\alpha(g)\leqslant\frac{1}{2}$, with the asymptotic behavior

$$\alpha(g)\simeq\begin{cases}\dfrac{1}{2}-\dfrac{3}{8}g & (g\to 0)\\[2ex] \dfrac{1}{\sqrt{3g}}-\dfrac{1}{3g} & (g\to\infty)\end{cases}.$$

Using Eq. (76), we can write for the approximations $f_k(g)$ the following expressions: in the zero order,

$$f_0(g)=-\frac{1}{2}\ln\alpha-\frac{3\alpha^2}{4(1-2\alpha)}, \tag{77}$$

where $\alpha=\alpha(g)$, in the first order,

$$f_1(g)=f_0(g)-\frac{1}{4}+\frac{1}{2}\alpha, \tag{78}$$

and in the second order,

$$f_2(g)=f_0(g)-\frac{1}{3}(1+5\alpha-14\alpha^2). \tag{79}$$

The zero-order approximation (77) correctly describes the weak- and strong-coupling limits of the exact function (61), but it is not accurate in the intermediate region. In this region, the behavior of the approximation

$$f_k(g)=f_0(g)+p_k(\alpha)$$

is governed by a series $p_k(\alpha)$ in powers of $\alpha=\alpha(g)$. Renormalizing this series twice, according to the bootstrap procedure [16], we obtain

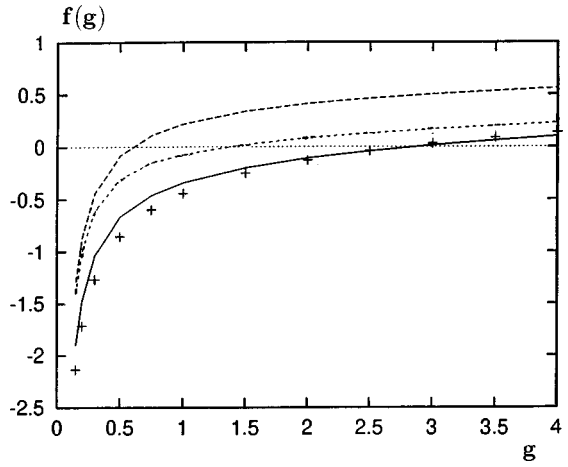


FIG. 1. The free energy of the double-well model given by the approximants $f_1(g)$ (dashed line), $f_2(g)$ (short-dashed line), and $f_2^*(g)$ (solid line). Crosses correspond to the exact values of function (61).

$$f_2^*(g)=f_0(g)-\frac{1}{3}\exp\left\{5\alpha\exp\left(-\frac{14}{5}\alpha\right)\right\}, \tag{80}$$

where $\alpha=\alpha(g)$ is given by Eq. (76). The obtained self-similar approximant (80) provides much better approximation to function (61), compared to $f_1(g)$ and $f_2(g)$. The crossing point $g_c^*=2.858$, defined by the condition $f_2^*(g_c^*)=0$, is quite close to the exact $g_c$ and gives an error 3.6%. That Eq. (80) is an accurate approximant is also clearly seen in Fig. 1.

### B. One-dimensional oscillator

From the model of the preceding section, we now pass to a more realistic case of the double-well oscillator with the Hamiltonian

$$H=-\frac{1}{2}\frac{d^2}{dx^2}+\frac{1}{16g}-\frac{1}{2}x^2+gx^4, \tag{81}$$

in which $x\in(-\infty,+\infty)$ and $g\in[0,\infty)$. The problem of finding the eigenvalues of Hamiltonian (81) is a challenge for any analytical method, although there are several numerical techniques calculating the eigenvalues with reasonable accuracy [38–43]. It is especially difficult to calculate the lowest energy levels. The main problem here is that instanton contributions are crucial in the weak-coupling region providing for an exponentially small splitting of energy levels. In addition, the energy of the ground-state level is not a monotone function of the coupling parameter $g$, which is also related to the instanton contributions. Below we shall consider the most difficult case of the ground-state energy and that of the first excited level separated from the former, in the weak-coupling region, by an exponentially small gap.

To construct interpolation formulas, we need asymptotic expansions for the weak- and strong-coupling limits. We shall use such expansions derived in Ref. [44]. The ground-state energy $e_+(g)$ corresponds to a symmetric wave function, while the first excited level, with an energy $e_-(g)$,

corresponds to an antisymmetric wave function. These energies can be written in the form

$$e_{\pm}(g)=\overline{e}(g)\mp\frac{1}{2}\Delta(g), \tag{82}$$

in which

$$\overline{e}(g)\equiv\frac{1}{2}[e_{+}(g)+e_{-}(g)], \quad \Delta(g)\equiv e_{-}(g)-e_{+}(g). \tag{83}$$

Let us notice that the Hamiltonian (81) is shifted, as compared to the standard form, by the term $1/16g$, which makes the spectrum of Eq. (81) everywhere positive [44].

For the average energy and the gap, defined in Eq. (83), we have [44] in the weak-coupling limit, when $g\rightarrow 0$,

$$\overline{e}(g)\simeq\frac{1}{\sqrt{2}}-\frac{21}{64}g \tag{84}$$

and, respectively,

$$\Delta(g)\simeq\frac{a}{g}\exp\left(\frac{b}{g}+c\right), \tag{85}$$

where

$$a=\frac{303}{1024}, \quad b=-\frac{\sqrt{2}}{4}, \quad c=\frac{9}{4}.$$

In the strong-coupling limit, when $g\rightarrow\infty$, we may derive [44] for the energies

$$e_{+}(g)\simeq\frac{3}{8}(6g)^{1/3}-\frac{1}{4}(6g)^{-1/3}+\frac{13}{12}(6g)^{-1}-\frac{2705}{3456}(6g)^{-5/3},$$

$$e_{-}(g)\simeq\frac{9}{8}(10)^{1/3}-\frac{3}{4}(10g)^{-1/3}+\frac{377}{144}(10g)^{-1}-\frac{159\,139}{31\,104}(10g)^{-5/3}.$$

From here, for the average energy we get

$$\overline{e}(g)\simeq Ag^{1/3}+Bg^{-1/3}+Cg^{-1}+Dg^{-5/3}, \tag{86}$$

where

$$A=1.552\,580, \quad B=-0.242\,850,$$

$$C=0.221\,181, \quad D=-0.074\,868.$$

And for the gap, we find

$$\Delta(g)\simeq A_1g^{1/3}+B_1g^{-1/3}+C_1g^{-1}+D_1g^{-5/3}, \tag{87}$$

where

$$A_1=1.742\,319, \quad B_1=-0.210\,539,$$

$$C_1=0.081\,250, \quad D_1=-0.070\,721.$$

Constructing a self-similar approximation from the right to the left, we have the right approximant

$$e_4^{*}(g,\infty)=\overline{e}^{*}(g)\mp\frac{1}{2}\Delta^{*}(g), \tag{88}$$

in which

$$\overline{e}^{*}(g)=\left[\frac{1}{4}+A^4g^{4/3}\exp\left(\frac{4B}{Ag^{2/3}}\right)\right]^{1/4}+\frac{Dg}{[g^{2/3}+(\frac{64}{21}|D|)^{1/4}]^4}. \tag{89}$$

The most difficult here is to interpolate between the power-law expansion (87) for the gap, in the strong-coupling limit, and the exponential behavior (85) in the weak-coupling region. Nevertheless, employing the technique of Sec. II, we obtain for the gap the form

$$\Delta^{*}(g)=\frac{\alpha^{*}(g)}{g}\exp\left\{\frac{\beta^{*}(g)}{g}\right\}, \tag{90}$$

describing a renormalized instanton contribution, where

$$\alpha^{*}(g)=\left[a^{3/2}+A_1^{3/2}g^2\exp\left\{\frac{3B_1}{2A_1g^{3/2}}\exp\left(\frac{C_1}{B_1g^{2/3}}\right)\right\}\right]^{2/3},$$

$$\beta^{*}(g)=\frac{|b|D_1}{[|D_1|^{4/3}+(|b|A_1)^{4/3}(\tau+g^{2/3})^{1/2}g]^{3/4}},$$

$$\tau\equiv 9\left(\frac{D_1^4}{A_1^4|b|^7}\right)^{2/3}=0.224\,17.$$

The behavior of two branches of Eq. (88), compared with the exact numerical data, correctly describes the nonmonotonic behavior of the ground-state energy and the exponential branching at $g=0$. The accuracy of the constructed formulas is very good for both the instanton-dominated region ($g\ll 0.2$) and instanton-free region ($g\gg 0.2$), with the error tending to zero in both these limits. The most difficult for description is a narrow intermediate region around the point $g\approx 0.2$, where an error is about 25%. The accuracy can be improved taking into account more terms of asymptotic expansions, but then the formulas become essentially more complicated.

### C. Quasistationary states

Quasistationary or resonance states are encountered in a variety of studies in atomic and molecular physics. A good discussion and many references are given in Ref. [45]. Several numerical calculations are known for this problem [6,42,45,46]. Here we derive analytical formulas for both the real and imaginary parts of the spectrum of the Hamiltonian

$$H=-\frac{1}{2}\frac{d^2}{dx^2}+\frac{1}{2}x^2-gx^4, \tag{91}$$

in which $x\in(-\infty,+\infty)$ and $g\in[0,\infty)$.

First, we have to analyze the asymptotic behavior of the spectrum in the weak- and strong-coupling limits. To this end, we invoke perturbation theory starting from the Hamiltonian

$$H_0=-\frac{1}{2}\frac{d^2}{dx^2}+\frac{u^2}{2}x^2, \tag{92}$$

in which $u$ is a trial parameter to be converted into a control function. Introducing, for convenience, the notation

$$E_k(g,u)\equiv\left(n+\frac{1}{2}\right)F_k(g,u) \tag{93}$$

of a $k$-order perturbative expression for the energy of a level $n=0,1,2,\ldots$, we find

$$F_0(g,u)=u, \quad F_1(g,u)=u-\frac{u}{4}(2\alpha-\beta),$$

$$F_2(g,u)=F_1(g,u)-\frac{u}{8}(\alpha^2-2\alpha\beta+2\beta^2\delta), \tag{94}$$

and so on, analogously to the case of the anharmonic oscillator [[13,31]], with the notation

$$\alpha\equiv 1-\frac{1}{u^2}, \quad \beta\equiv-\frac{6\gamma g}{u^3}, \quad \gamma\equiv\frac{n^2+n+1/2}{n+1/2},$$

$$\delta\equiv\frac{17n^2+17n+21}{(6\gamma)^2}.$$

The control function $u=u(g)$ can be defined from the fixed-point condition

$$\frac{\partial}{\partial u}F_k(g,u)=0. \tag{95}$$

In the first order, we get the equation

$$u^3-u+6\gamma g=0, \tag{96}$$

as a result of which

$$\alpha=\beta=\frac{u^2-1}{u^2}.$$

Substituting the solution $u(g)$ to Eq. (96) into Eq. (94), we define

$$f_k(g)\equiv F_k(g,u(g)). \tag{97}$$

Then, from Eq. (94) we have

$$f_1(g)=\frac{3}{4}u+\frac{1}{4u}, \quad f_2(g)=f_1(g)+\frac{1}{8}(1-2\delta)\alpha^2 u. \tag{98}$$

From three solutions of Eq. (96) we need to choose that which satisfies the boundary condition $u(g)\to 1$, as $g\to 0$. Such a solution is

$$u(g)=\left(\frac{1}{9}\sqrt{729\gamma^2g^2-3}-3\gamma g\right)^{1/3}+\frac{1}{3}\left(\frac{1}{9}\sqrt{729\gamma^2g^2-3}-3\gamma g\right)^{-1/3}. \tag{99}$$

The control function (99) is real for $g\leqslant g_n$, where

$$g_n\equiv\frac{g_0}{\gamma}=\frac{n+1/2}{n^2+n+1/2}g_0, \quad g_0\equiv\frac{\sqrt{3}}{27}=0.064\,150. \tag{100}$$

Complex roots of Eq. (99) appear only after $g>g_n$. The fact that Im $u_k(g)=0$ for $g\leqslant g_n$ leads to Im $f_k(g)=0$, when $g\leqslant g_n$.

Asymptotic expansions in the weak- and strong-coupling limits can be written for arbitrary energy levels. For illustrative purpose, we shall write down expansions for the ground state $(n=0)$ and the first excited state $(n=1)$.

For the ground state, when $n=0$ and $\gamma=1$, function (98) yields for the real parts

$$\text{Re } f_1(g)\simeq 1-\frac{3}{2}-\frac{9}{2}g^2-27g^3-\frac{1701}{8}g^4,$$

$$\text{Re } f_2(g)\simeq 1-\frac{3}{2}g-\frac{21}{4}g^2-\frac{153}{4}g^3-\frac{729}{2}g^4 \quad (n=0), \tag{101}$$

while the imaginary parts are

$$\text{Im } f_1(g)=\text{Im } f_2(g)=0, \quad g\to 0. \tag{102}$$

For the first excited level, for which $n=1$ and $\gamma=5/3$, for the real parts of Eq. (98) we find

$$\text{Re } f_1(g)\simeq 1-\frac{5}{2}g-\frac{25}{2}g^2-125g^3-\frac{13\,125}{8}g^4,$$

$$\text{Re } f_2(g)\simeq 1-\frac{5}{2}g-\frac{55}{4}g^2-\frac{625}{4}g^3-\frac{9375}{4}g^4 \quad (n=1), \tag{103}$$

while their imaginary parts are again as in Eq. (102).

In the strong-coupling limit, when $g\to\infty$, for the ground state we obtain the real parts

$$\text{Re } f_1(g)\simeq\frac{3}{8}(6g)^{1/3}+\frac{1}{4}(6g)^{-1/3}+\frac{1}{12}(6g)^{-1}+\frac{1}{108}(6g)^{-5/3}-\frac{1}{648}(6g)^{-7/3},$$

$$\text{Re } f_2(g)\simeq\frac{35}{96}(6g)^{1/3}+\frac{77}{288}(6g)^{-1/3}+\frac{17}{144}(6g)^{-1}+\frac{43}{1944}(6g)^{-5/3}-\frac{211}{23\,328}(6g)^{-7/3}, \tag{104}$$

and the imaginary parts

$$\mathrm{Im}\, f_1(g) \simeq -\frac{3\sqrt{3}}{8}(6g)^{1/3}+\frac{\sqrt{3}}{4}(6g)^{-1/3}-\frac{\sqrt{3}}{108}(6g)^{-5/3} -\frac{\sqrt{3}}{648}(6g)^{-7/3},$$

$$\mathrm{Im}\, f_2(g) \simeq -\frac{35\sqrt{3}}{96}(6g)^{1/3}+\frac{77\sqrt{3}}{288}(6g)^{-1/3} -\frac{43\sqrt{3}}{1944}(6g)^{-5/3}-\frac{211\sqrt{3}}{23\,328}(6g)^{-7/3}. \tag{105}$$

For the strong-coupling limit, in the case of the first excited level ($n=1$), we find the real parts

$$\mathrm{Re}\, f_1(g) \simeq \frac{3}{8}(10g)^{1/3}+\frac{1}{4}(10g)^{-1/3}+\frac{1}{12}(10g)^{-1} +\frac{1}{108}(10g)^{-5/3}-\frac{1}{648}(10g)^{-7/3},$$

$$\mathrm{Re}\, f_2(g) \simeq \frac{59}{160}(10g)^{1/3}+\frac{25}{96}(10g)^{-1/3}+\frac{5}{48}(10g)^{-1} +\frac{11}{648}(10g)^{-5/3}-\frac{47}{7776}(10g)^{-7/3}, \tag{106}$$

and imaginary parts

$$\mathrm{Im}\, f_1(g) \simeq -\frac{3\sqrt{3}}{8}(10g)^{1/3}+\frac{\sqrt{3}}{4}(10g)^{-1/3}-\frac{\sqrt{3}}{108}(10g)^{-5/3} -\frac{\sqrt{3}}{648}(10g)^{-7/3},$$

$$\mathrm{Im}\, f_2(g) \simeq -\frac{59\sqrt{3}}{160}(10g)^{1/3}+\frac{25\sqrt{3}}{96}(10g)^{-1/3} -\frac{11\sqrt{3}}{648}(10g)^{-5/3}-\frac{47\sqrt{3}}{7776}(10g)^{-7/3}. \tag{107}$$

The accuracy of the real parts of the approximations in Eq. (98) is sufficiently good; the maximal error in the first order is $-3.3\%$ and that of the second order is $2\%$. In the case of the corresponding imaginary parts, the maximal error for $g>g_n$ is on the order of 10%. However, for $g\leqslant g_n$, imaginary parts are identically zero, because of which their weak-coupling expansions do not exist.

To correct the described deficiency, let us consider the fixed-point condition (95) of second order. Then, the equation for the control function becomes of the form

$$u^6-2u^4+16\gamma g u^3+u^2-16\gamma g u+120\gamma^2\delta g^2=0. \tag{108}$$

For the ground-state level, for which $n=0$, $\gamma=1$, and $\delta=7/12$, Eq. (108) reduces to

$$u^6-2u^4+16gu^3+u^2-16gu+70g^2=0. \tag{109}$$

The solution to Eq. (109) will be denoted by $u^*(g)$, in order to distinguish it from that of Eq. (96). Among the solutions of Eq. (109) it is necessary to choose that which satisfies the asymptotic boundary condition $u^*(g)\to 1$, as $g\to 0$. Substituting $u^*(g)$ into

$$F_2(g,u)=\frac{3}{8}u+\frac{3}{4u}-\frac{3g}{u^2}-\frac{1}{8u^3}+\frac{3g}{2u^4}-\frac{21g^2}{4u^5},$$

we come to

$$f_2^*(g)\equiv F_2(g,u^*(g)). \tag{110}$$

Defining the real and imaginary parts of Eq. (110), we take those of them for which

$$\mathrm{Re}\, f_k^*(g)>0, \quad \mathrm{Im}\, f_k^*(g)\leqslant 0.$$

To solve Eq. (109), we introduce a new variable

$$\lambda\equiv u(u^2-1), \tag{111}$$

for which Eq. (109) reduces to a much simpler equation

$$\lambda^2+16g\lambda+70g^2=0. \tag{112}$$

From two solutions to this equation, $\lambda_{1,2}=-(8\pm i\sqrt{6})g$, we need to choose such that, together with Eq. (111), gives the control function $u^*(g)$ satisfying the conditions discussed above. The desired solution to Eq. (112) is

$$\lambda(g)=-(8+i\sqrt{6})g. \tag{113}$$

Then from the equation $u^3-u-\lambda=0$ we find

$$u^*(g)=\left(\frac{\lambda}{2}+\frac{1}{18}\sqrt{81\lambda^2-12}\right)^{1/3} +\frac{1}{3}\left(\frac{\lambda}{2}+\frac{1}{18}\sqrt{81\lambda^2-12}\right)^{-1/3}, \tag{114}$$

where $\lambda=\lambda(g)$ is defined in Eq. (113).

In the weak-coupling limit, when $g\to 0$ together with $\lambda\to 0$, approximant (110) has the following asymptotic expansions for the real part:

$$\mathrm{Re}\, f_2^*(g) \simeq 1-\frac{3}{2}g-\frac{21}{4}g^2-41g^3-\frac{14\,157}{32}g^4-5547g^5 -\frac{9\,441\,289}{128}g^6, \tag{115}$$

and for the imaginary part

$$\mathrm{Im}\, f_2^*(g) \simeq -\frac{3}{4}\sqrt{6}g^3-27\sqrt{6}g^4-\frac{1413}{2}\sqrt{6}g^5-\frac{64\,779}{4}\sqrt{6}g^6. \tag{116}$$

In the strong-coupling limit, when $g\to\infty$ and $|\lambda|\to\infty$, for the real part of Eq. (110), we have

TABLE III. The double energy $f_2^*(g)=2E^*(g)$ of the lowest quasistationary state, as compared to numerical values $f(g)$.

| $g$ | $\mathrm{Re}f(g)$ | $\mathrm{Re}f_2^*(g)$ | $-\mathrm{Im}f(g)$ | $-\mathrm{Im}f_2^*(g)$ |
|---|---|---|---|---|
| 0.01 | 0.984428 | 0.984429 | 0.000000 | 0.000003 |
| 0.02 | 0.967451 | 0.967477 | 0.000001 | 0.000035 |
| 0.05 | 0.900673 | 0.901116 | 0.006693 | 0.004888 |
| 0.1 | 0.794881 | 0.791404 | 0.089412 | 0.090883 |
| 0.2 | 0.72882 | 0.728985 | 0.27735 | 0.281642 |
| 0.5 | 0.7477 | 0.751513 | 0.6100 | 0.613077 |
| 1.0 | 0.8297 | 0.834876 | 0.9097 | 0.911547 |
| 2.0 | 0.964 | 0.971001 | 1.260 | 1.261483 |
| 5.0 | 1.23 | 1.238149 | 1.84 | 1.832649 |

$$\mathrm{Re}\, f_2^*(g)\simeq 0.672\,436g^{1/3}+0.145\,202g^{-1/3}+0.016\,735g^{-1}+0.000\,603g^{-5/3}-0.000\,088g^{-7/3}-0.000\,010g^{-3}-0.7\times 10^{-7}g^{-11/3}, \tag{117}$$

and for its imaginary part, we find

$$\mathrm{Im}\, f_2^*(g)\simeq -1.155\,930g^{1/3}+0.246\,594g^{-1/3}-0.000\,750g^{-1}-0.001\,364g^{-5/3}-0.000\,101g^{-7/3}+0.000\,003g^{-3}+0.000\,001g^{-11/3}. \tag{118}$$

The approximant (110) possesses the weak-coupling expansion for its imaginary part, thus correcting the deficiency of the approximations in Eq. (98). The values of the real and imaginary parts of $f_2^*(g)$ for different $g$, as compared to the precise numerical calculations [42,47], are given in Table III. The maximal percentage error of the real part is 0.7%. The percentage error of the imaginary part cannot be correctly defined, since $\mathrm{Im}\, f(g)\to 0$ as $g\to 0$. Recall that the ground-state energy $E(g)$ for Hamiltonian (91) is related, according to Eq. (93), with the function $f(g)$ as

$$E(g)=\frac{1}{2}f(g). \tag{119}$$

To write an analytical formula approximating $f(g)$ in the whole range of the parameter $g\in[0,\infty)$, we may use the asymptotic expansions derived above. Employing the technique of Sec. II, we can obtain for the real part the approximants

$$\mathrm{Re}\, f_2^*(g,0)=[\exp(-6a_1g)+A_1^6g^2]^{1/6}, \tag{120}$$

$$\mathrm{Re}\, f_3^*(g,0)=[\exp\{-6(a_1+a_2)g\}+A_1^6g^2]^{1/6}+a_2g\left[1+\left(\frac{a_2}{A_2}\right)^{3/2}g^2\right]^{2/3}, \tag{121}$$

in which

$$a_1=1.5,\quad a_2=0.548,\quad A_1=0.672\,436,\quad A_2=0.145\,202.$$

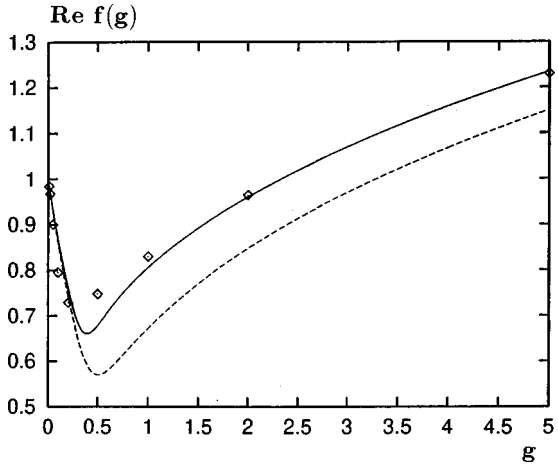


FIG. 2. The real part of the double energy for the lowest quasiresonance state represented by the approximants $\mathrm{Re}f_2^*(g,0)$ (dashed line) and $\mathrm{Re}f_3^*(g,0)$ (solid line), compared to exact values marked by diamonds.

The behavior of these approximants is shown in Fig. 2. The maximal percentage error of $f_2^*(g,0)$ is 24% and that of $f_3^*(g,0)$ is 9%.

To reach good accuracy for the imaginary part, we need to consider higher-order approximations. For the imaginary part we find the following sequence of self-similar approximants:

$$\mathrm{Im}\, f_3^*(g,0)=-ag^3\left[\exp\left(-\frac{3b}{4a}g\right)+\left(\frac{a}{A}\right)^{3/4}g^2\right]^{-4/3}, \tag{122}$$

where $a=\frac{3}{4}\sqrt{6}$, $b=27\sqrt{6}$, and $A=1.155\,930$,

$$\mathrm{Im}\, f_4^*(g,0)=-ag^3\left\{\left[\exp\left(-\frac{27b}{28a}g\right)+\frac{27}{28}B_1g^2\right]^{7/6}+\left(\frac{a}{A}\right)^{9/8}g^3\right\}^{-8/9}, \tag{123}$$

where $a$, $b$, and $A$ are the same as in Eq. (122) and $B_1=0.477\,045$,

$$\mathrm{Im}\, f_5^*(g,0)=-ag^3\left(\left\{\left[\exp\left(-\frac{81b}{70a}g\right)+\frac{81}{70}B_2g^2\right]^{7/6}+\frac{27}{20}B_3g^3\right\}^{10/9}+\left(\frac{a}{A}\right)^{3/2}g^4\right)^{-2/3}, \tag{124}$$

where $B_2=0.178\,716$ and $B_3=0.496\,502$,

$$\mathrm{Im}\, f_6^*(g,0)=-ag^3\left[\left(\left\{\left[\exp\left(-\frac{243b}{182a}g\right)+\frac{243}{182}B_4g^2\right]^{7/6}+\frac{81}{52}B_5g^3\right\}^{10/9}+\frac{45}{26}B_6g^4\right)^{13/12}+\left(\frac{a}{A}\right)^{15/8}g^5\right]^{-8/15}, \tag{125}$$

where $B_4=0.073\,553$, $B_5=0.196\,401$, and $B_6=0.552\,922$.

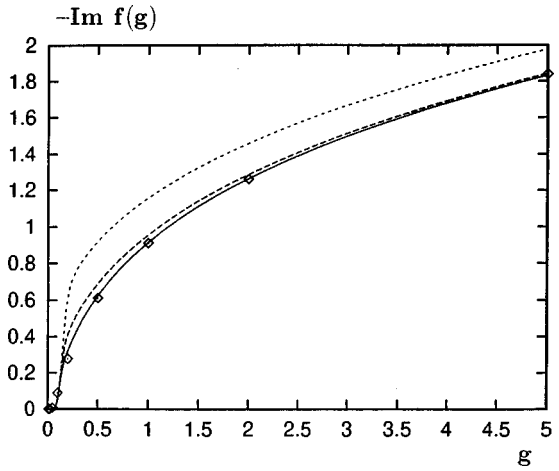


FIG. 3. The modulus of the imaginary part of the double energy for the lowest quasiresonance state given by the approximants $\mathrm{Im}f_3^*(g,0)$ (short-dashed line), $\mathrm{Im}f_4^*(g,0)$ (dashed line), and $\mathrm{Im}f_6^*(g,0)$ (solid line). Exact data are shown by diamonds.

The behavior of the self-similar approximants (122)–(125) is displayed in Fig. 3. The curves corresponding to Eqs. (124) and (125) almost coincide in this picture. Figure 3 clearly demonstrates the convergence of the sequence $\{\mathrm{Im}\ f_k^*(g,0)\}$ to exact data marked by diamonds.

## V. NONLINEAR HAMILTONIANS

Here we show that our approach is applicable not only to linear problems of quantum mechanics but to nonlinear problems as well.

### A. One-dimensional case

Consider the nonlinear Hamiltonian

$$H=-\frac{1}{2}\frac{d^2}{dx^2}+\frac{1}{2}x^2+g\psi^2(x), \tag{126}$$

in which $x\in(-\infty,+\infty)$, $g\in(-\infty,+\infty)$, and $\psi(x)$ is a wave function.

The Hamiltonian (126) is a prototype of the $\varphi^4$ model of quantum field theory. There exists a controversy in the interpretation of the so-called ''triviality'' of this theory (see discussion in Refs. [48–50]). Therefore, developing methods that could successfully deal with nonlinear Hamiltonians of the type (126) could be useful for $\varphi^4$ quantum field theories, as well as for those field theories that include scalar-field terms, like Eq. (126), in their Lagrangians, e.g., as in the Higgs model [51]. Another important application of the nonlinear Hamiltonian of the form (126) is for describing properties of atoms confined in magnetic traps [52–54]. Such magnetically trapped atoms of $^{87}$Rb, $^{23}$Na, and $^{7}$Li, as has been observed recently [55–57], can exhibit the phenomenon of Bose-Einstein condensation. The possibility of the direct observation of Bose condensation distinguishes these alkali-metal gases from liquid $^4$He where this condensation could be investigated only indirectly (see the related discussion in Refs. [58–63]). The system of condensed trapped atoms corresponds to the ground state of the Hamiltonian (126). We consider here the one-dimensional case which serves as an illustration of the applicability of the method.

It is worth emphasizing that the coupling parameter $g$ in Eq. (126), when a system of $N$ condensed atoms is considered, is proportional to $N$. Because of this, for $N\gg 1$, the coupling parameter can become large and, consequently, perturbation theory in powers of $g$ is of no sense. Although some thermodynamic characteristics of trapped atoms can be approximately analyzed disregarding their interactions, that is, nonlinearity [64–67], but a correct description certainly has to take into account these interactions [68], i.e., nonlinearity, since for the cases related to experiment [55–57] the effective coupling is strong, $g\gg 1$.

To derive analytical formulas for the spectrum of the Hamiltonian (126), we need to find appropriate asymptotic expansions. Let us start with the Hamiltonian

$$H_0=-\frac{1}{2}\frac{d^2}{dx^2}+\frac{u^2}{2}x^2, \tag{127}$$

in which $u$ is a trial parameter. Employing perturbation theory with respect to the perturbation

$$\Delta H=\frac{1}{2}(1-u^2)x^2+g\psi^2(x),$$

we may find the $k$-order approximation

$$E_k(g,u)=\left(n+\frac{1}{2}\right)F_k(g,u) \tag{128}$$

for the energy levels labeled by $n=0,1,2,\ldots$ . For the function $F_k$ defined in Eq. (128) we have

$$F_0(g,u)=u,\quad F_1(g,u)=\frac{1}{2}\left(u+\frac{1}{u}\right)+\frac{J_n}{n+1/2}g\sqrt{u}, \tag{129}$$

where

$$J_n=\frac{1}{\pi 2^n n!}\int_{-\infty}^{+\infty}\exp(-2x^2)H_n^4(x)dx,$$

$H_n(x)$ being a Hermite polynomial. In particular,

$$J_0=\frac{1}{\sqrt{2\pi}},\quad J_1=\frac{3}{4\sqrt{2\pi}},\quad J_2=\frac{41}{64\sqrt{2\pi}}.$$

The control function $u=u(g)$ can be found from the fixed-point condition

$$\frac{\partial}{\partial u}F_1(g,u)=0. \tag{130}$$

The latter, with the notation

$$\alpha\equiv\frac{J_n}{n+1/2}g, \tag{131}$$

yields

$$u^2+u^{3/2}\alpha-1=0. \tag{132}$$

Substituting the solution $u(g)$ to Eq. (132) into Eq. (129), we get

$$f_k(g)=F_k(g,u(g)). \tag{133}$$

For instance,

$$f_1(g)=\frac{1}{2}\left(\frac{3}{u}-u\right), \quad u=u(g). \tag{134}$$

In the weak-coupling limit, $\alpha\to 0$ when $g\to 0$, according to Eq. (131). Then Eq. (134) gives

$$f_1(g)\simeq 1+\alpha-\frac{1}{8}\alpha^2+\frac{1}{32}\alpha^3-\frac{1}{128}\alpha^4+\frac{3}{2048}\alpha^5. \tag{135}$$

In the strong-coupling limit, when $g\to\infty$ together with $\alpha\to\infty$, Eq. (134) leads to

$$f_1(g)\simeq\frac{3}{2}\alpha^{2/3}+\frac{1}{2}\alpha^{-2/3}-\frac{1}{6}\alpha^{-2}+\frac{7}{54}\alpha^{-10/3}. \tag{136}$$

In the case of a negative coupling parameter $g<0$, the weak-coupling limit, when $g\to -0$ and $\alpha\to -0$, gives the same asymptotic expansion as Eq. (135). However, the strong-coupling limit, when $g\to -\infty$ and $\alpha\to -\infty$, is different from Eq. (136). If $\alpha\to -\infty$, then Eq. (134) behaves as

$$f_1(g)\simeq -\frac{\alpha^2}{2}+\frac{1}{2\alpha^2}-\frac{1}{2\alpha^6}+\frac{3}{2\alpha^{10}}-\frac{13}{2\alpha^{14}}. \tag{137}$$

In the region of negative $g<0$, the energy (128) is positive for small $|g|$, and, as $g$ diminishes, the energy becomes zero at a critical value $g_c$. The latter can be found from the definition

$$f_1(g_c)=0. \tag{138}$$

The form (134) shows that equality (138) holds true for $u_c^2=3$. Then, Eq. (132) immediately gives

$$\alpha_c=-\frac{2}{3^{3/4}}=-0.877\,38. \tag{139}$$

Because of the relation (131), one has

$$g_c=-\left(n+\frac{1}{2}\right)\frac{\alpha_c}{J_n}. \tag{140}$$

For example, for the ground-state level, with $n=0$, one finds

$$g_c=-1.099\,64 \quad (n=0). \tag{141}$$

For $g<g_c$, the energy becomes negative, which implies the instability of the system.

Note that invoking the notation (131), we have managed to write the asymptotic expansions (135), (136), and (137) for arbitrary energy levels. Using the derived expansions, we can construct analytical formulas for the whole spectrum of the considered nonlinear Hamiltonian. Thus, following the standard way of Sec. II, we find for $\alpha\geq 0$ the approximant

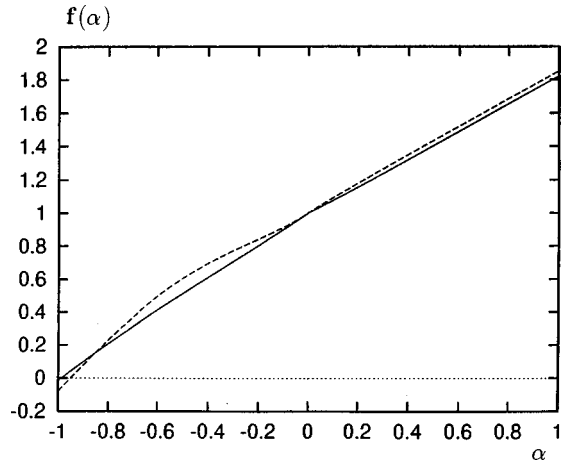


FIG. 4. The self-similar approximants $f_2^*(\alpha,0)$ (solid line) and $f_2^*(\alpha,\infty)$ (dashed line) for $\alpha\geq 0$ and the approximants $f_2^*(\alpha,-0)$ (solid line) and $f_3^*(\alpha,-\infty)$ (dashed line) for $\alpha\leq 0$, in the region $-1\leq\alpha\leq 1$.

$$f_2^*(\alpha,0)=[(1+a_1A_1^3\sqrt{8A_2^3}\alpha)^{2/3}+A_1^3\alpha^2]^{1/3}, \tag{142}$$

where $a_1=1$, $A_1=3/2$, and $A_2=1/2$. Similarly, we can write down

$$f_2^*(\alpha,\infty)=\left[1+A_1^4\alpha\left(\frac{16A_2}{5A_1}\tau_2+\alpha^{4/3}\right)^{5/4}\right]^{1/4}, \tag{143}$$

where $A_1$ and $A_2$ are the same as before and

$$\tau_2=\frac{5}{A_2}\left(\frac{a_1^4}{2^{12}A_1^{11}}\right)^{1/5}=0.776.$$

For $\alpha\leq 0$, we may construct

$$f_2^*(\alpha,-0)=1+a_1\alpha\left[\exp\left(-\frac{2a_2}{a_1}\alpha\right)+\frac{B_1^2}{a_1^2}\alpha^2\right]^{1/2}, \tag{144}$$

with $a_2=-1/8$ and $B_1=-1/2$. Another approximant is

$$f_3^*(\alpha,-\infty)=B_1\alpha^2+B_2\left[B_2^4+|\alpha|\left(\alpha^4-\frac{16B_3}{7B_2}\tau_3\right)^{7/4}\right]^{-1/4}, \tag{145}$$

where $B_2=1/2$, $B_3=-1/2$, and

$$\tau_3=\frac{7}{|B_3|}\left(\frac{a_1^4B_2^{23}}{2^{20}}\right)^{1/7}=0.198.$$

The behavior of approximants (142)–(145) is such that $f_2^*(\alpha,0)$ practically coincides with $f_2^*(\alpha,\infty)$ for $\alpha\geq 0$, while $f_2^*(\alpha,-0)$ coincides with $f_3^*(\alpha,-\infty)$ for $\alpha\leq 0$. A slight difference between these approximants is noticeable only in the region $-1\leq\alpha\leq 1$, as is shown in Fig. 4.

### B. Radial model

In the preceding section we considered a one-dimensional nonlinear problem. It is straightforward to apply the same

approach to nonlinear problems of higher dimensionalities. As an illustration, we consider a spherically symmetric model with the nonlinear radial Hamiltonian

$$H=-\frac{1}{2}\frac{d^2}{dr^2}+\frac{l(l+1)}{2r^2}+\frac{1}{2}r^2+gR_{nl}^2(r), \qquad (146)$$

in which $r\in[0,\infty)$, $n=0,1,2,\ldots$, $l=0,1,2,\ldots$, the coupling parameter $g\in(-\infty,+\infty)$, and $R_{nl}$ is a radial wave function.

Starting from the trial Hamiltonian

$$H_0=-\frac{1}{2}\frac{d^2}{dr^2}+\frac{l(l+1)}{2r^2}+\frac{u^2}{2}r^2, \qquad (147)$$

with a trial parameter $u$, we invoke perturbation theory with respect to the perturbation $\Delta H=H-H_0$. For the $k$-order approximation of the spectrum we may write

$$E_k(g,u)\equiv\left(2n+l+\frac{3}{2}\right)F_k(g,u). \qquad (148)$$

Introduce the effective coupling parameter

$$\alpha\equiv\frac{J_{nl}}{2n+l+3/2}g, \qquad (149)$$

in which

$$J_{nl}=\left[\frac{2n!}{\Gamma(n+l+3/2)}\right]^2\int_0^\infty r^{4(l+1)}e^{-2r^2}[L_n^{l+1/2}(r^2)]^4dr,$$

where $\Gamma$ is a gamma function and $L_n^l$ is an associated Laguerre polynomial. For the particular cases that will be analyzed in what follows, we have

$$J_{00}=\frac{3}{2\sqrt{2\pi}},\quad J_{01}=\frac{35}{24\sqrt{2\pi}},\quad J_{10}=\frac{147}{128\sqrt{2\pi}},$$

$$J_{02}=\frac{231}{160\sqrt{2\pi}}.$$

Accomplishing the same steps as in the preceding section, we can find the spectrum

$$e_{nl}(g)=\left(2n+l+\frac{3}{2}\right)f_1(g), \qquad (150)$$

in which $f_1(g)$ is defined identically to Eq. (133). The control function $u(g)$ is given by the solution of Eq. (132), only with $\alpha$ introduced in Eq. (149). With this renotation for the parameter $\alpha$, all asymptotic expansions for $f_1(g)$ are the same as in Sec. VII. Therefore the corresponding approximants $f_k^*$ will have the same forms (142)–(145).

What differentiates the considered nonlinear radial model from the one-dimensional nonlinear case is that the energy levels are labeled now by two quantum indices, $n$ and $l$. For some combinations of these indices, the specific effect of *level crossing*, when varying $g$, may occur. To illustrate this, let us analyze several lower levels of the spectrum (150). In the weak-coupling limit we may find

$$e_{00}\simeq\frac{3}{2}\left(1+\frac{g}{\sqrt{2\pi}}\right),\quad e_{01}\simeq\frac{5}{2}\left(1+\frac{7g}{12\sqrt{2\pi}}\right),$$

$$e_{10}\simeq\frac{7}{2}\left(1+\frac{21g}{64\sqrt{2\pi}}\right),\quad e_{02}\simeq\frac{7}{2}\left(1+\frac{33g}{80\sqrt{2\pi}}\right),\quad g\to 0$$

while for the strong-coupling limit, we have

$$e_{00}(g)\simeq 1.219\,334g^{2/3},\quad e_{10}(g)\simeq 1.353\,502g^{2/3},$$

$$e_{01}(g)\simeq 1.418\,783g^{2/3},\quad e_{02}(g)\simeq 1.576\,577g^{2/3},\quad g\to\infty.$$

As is seen, at small $g$ the energy level $e_{01}$ is lower than $e_{10}$, but at large $g$, vice versa, the level $e_{10}$ becomes lower than $e_{01}$.

Another difference with the one-dimensional nonlinear case is the value of the critical coupling constant $g_c$ at which the energy level $e_{nl}(g)$ crosses zero. This critical parameter is defined as in Eq. (138) and gives the same $\alpha_c$ as in Eq. (139). But, because of the different relation (149) between $\alpha$ and $g$, we now get, instead of Eq. (140), the critical coupling

$$g_c=-\left(2n+l+\frac{3}{2}\right)\frac{\alpha_c}{J_{nl}}.$$

For the ground-state level, instead of Eq. (141), we find

$$g_c=-2.199\,27\quad(n=l=0),$$

so that $|g_c|$ is about twice larger than that for the one-dimensional case.

## VI. WAVE FUNCTIONS

In this section we show that the approach we have developed permits us to construct analytical expressions not only for energy levels but for wave functions as well. We shall concentrate our attention on the most interesting, from our point of view, case of nonlinear equations.

### A. Nonlinear Schrödinger equation

Consider the equation

$$-\frac{1}{2}\frac{d^2\psi}{dx^2}+\frac{1}{2}x^2\psi+g\psi^3=E\psi, \qquad (151)$$

in which $x\in(-\infty,+\infty)$ and $g\in[0,\infty)$. The nonlinear Schrödinger equations of this type are used for describing Bose-condensed atoms in magnetic traps [55–57]. This kind of equations is also often called the Gross-Ginzburg-Pitaevskii equation [69–72]. Condensed atoms correspond to the ground state of Eq. (151), which is assumed in what follows.

The wave function $\psi=\psi(x)$ is normalized by the condition

$$\int_{-\infty}^{+\infty}|\psi(x)|^2dx=1. \qquad (152)$$

From Eq. (151) it follows that the wave function is an even function, so that $\psi(x)=\psi(-x)$. Because of this, it has an expansion

$$\psi(x)\simeq c_0+c_2x^2+c_4x^4, \tag{153}$$

as $x\rightarrow 0$, in even powers of $x$. For large $x$, the harmonic term in Eq. (151) becomes predominant, and the wave function has the asymptotic behavior

$$\psi(x)\simeq A\exp\left(-\frac{1}{2}x^2\right) \tag{154}$$

as $x\rightarrow\infty$. Our aim is to find an analytical expression for $\psi(x)$ valid in the whole region of $x\in(-\infty,+\infty)$. Note that Padé approximants are not able to interpolate between such different types of behavior as the power law in Eq. (153) and exponential in Eq. (154). But using the self-similar interpolation of Sec. II, we easily obtain the self-similar approximant

$$\psi^*(x)=A\exp\left\{-\frac{1}{2}x^2+ax^2\exp(-bx^2)\right\}, \tag{155}$$

where $\psi^*(x)\equiv\psi_3^*(x,0)$ and

$$A=c_0, \quad a=\frac{1}{2}+\frac{c_2}{c_0}, \quad b=-\frac{c_4}{ac_0^2}.$$

Expression (155) acquires a transparent physical meaning when written in the form

$$\psi^*(x)=A\exp\left\{-\frac{x^2}{\xi^2(x)}\right\},$$

in which

$$\xi(x)=\left(\frac{1}{2}-a\exp\{-bx^2\}\right)^{-1/2}$$

plays the role of an effective correlation length.

The parameters $a$, $b$, and $A$ in Eq. (155) are not independent. The relation between them can be found if we expand Eq. (155) in powers of $x$ and substitute this expansion into Eq. (151). For small $x$, Eq. (155) gives

$$\psi^*(x)\simeq c_0+c_2x^2+\overline{c_4}x^4 \quad (x\rightarrow 0),$$

where $\overline{c_4}=c_4+c_2^2/2c_0$. Substituting this into Eq. (151) and equating the terms at like powers of $x$, we find the relations

$$c_2=c_0(gc_0^2-E), \quad c_4=\frac{c_0}{12}(1+4gc_0^2E-4E^2). \tag{156}$$

The latter yield the equalities

$$a=\frac{1}{2}+gA^2-E, \quad b=\frac{2(1-2a)E-1}{12aA} \tag{157}$$

showing that among four parameters, $a$, $b$, $A$, and $E$, only two are independent. Two additional equations for defining all parameters are the normalization condition (152) and the definition of the energy

$$E^*(g)=(\psi^*,H\psi^*), \tag{158}$$

where the Hamiltonian $H$ is the same as in Eq. (126) and the notation $E^*(g)\equiv E$ stresses that the energy is obtained by using the self-similar approximant (155).

The values of $a$, $b$, and $E^*$ depend on the coupling parameter $g$. Thus, for the weak-coupling limit $g\rightarrow 0$ we have

$$E^*(g)\simeq\frac{1}{2}+\frac{1}{\sqrt{2\pi}}g, \quad A^2=c_0^2\simeq\frac{1}{\sqrt{\pi}}.$$

Then, relations (156) give

$$\frac{c_2}{c_0}\simeq-\frac{1}{2}+\frac{\sqrt{2}-1}{\sqrt{2\pi}}g, \quad \frac{c_4}{c_0}\simeq-\frac{\sqrt{2}-1}{b\sqrt{\pi}}g.$$

Respectively, from Eq. (157) we get

$$a\simeq\frac{\sqrt{2}-1}{\sqrt{2\pi}}g=0.165\,247g, \quad b\simeq\frac{1}{3\sqrt{2}}=0.235\,702.$$

This demonstrates that the function (155) reduces to the Gaussian form when $g\rightarrow 0$.

The variational Gaussian function

$$\psi_G(x)=\left(\frac{u}{\pi}\right)^{1/4}\exp\left(-\frac{u}{2}x^2\right) \tag{159}$$

is often used not only for small $g\ll 1$ but for arbitrary $g\in[0,\infty)$, with the effective frequency $u=u(g)$ defined by the minimum of the energy $(\psi_G,H\psi_G)$, which gives

$$u^2+u^{3/2}\sqrt{\frac{2}{\pi}}g-1=0.$$

Such a variational energy is very close, with a deviation not more than several percent, to the energy

$$E_2^*(g)=\frac{1}{2}f_2^*(\alpha,0), \quad \alpha\equiv\sqrt{\frac{2}{\pi}}g,$$

corresponding to Eq. (142), which results in

$$E_2^*(g)=\frac{1}{2}\left[\left(1+\frac{27}{4\sqrt{2\pi}}g\right)^{2/3}+\frac{27}{4\pi}g^2\right]^{1/3}. \tag{160}$$

Another very often used approximation for treating Bose-condensed atoms in harmonic traps is the Thomas-Fermi approximation (see, e.g., [73–75]), which for Eq. (151) leads to the wave function

$$\psi_{\rm TF}(x)=\left(\frac{x_0^2-x^2}{2g}\right)^{1/2}, \quad |x|\leqslant x_0$$

$$\psi_{\rm TF}(x)=0, \quad |x|\geqslant x_0 \tag{161}$$

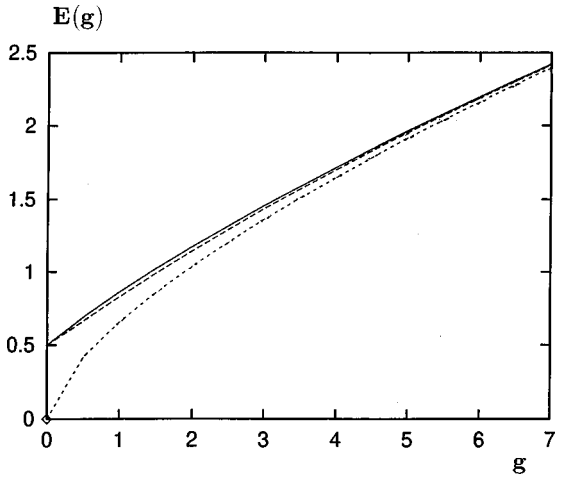


FIG. 5. The ground-state energy for the nonlinear Schrödinger equation (151) for the self-similar approximants $E^*(g)$ (solid line) and $E_2^*(g)$ (dashed line) and for the Thomas-Fermi approximation $E_{\rm TF}(g)$ (short-dashed line).

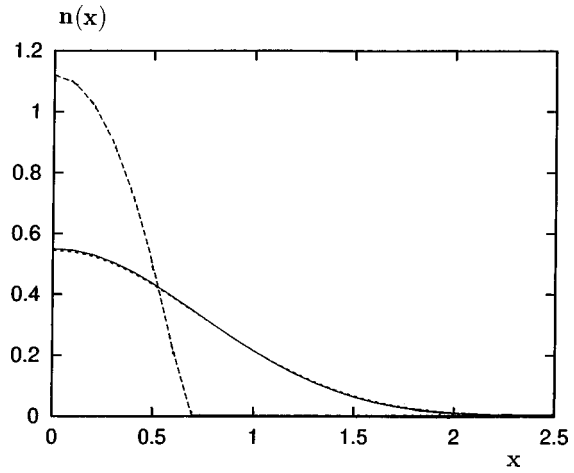


FIG. 6. The density (163) for the corresponding wave functions in the self-similar approximation (155) (solid line), Gaussian approximation (159) (short-dashed line), and Thomas-Fermi approximation (dashed line) for $g=0.2$.

in which

$$x_0 \equiv \sqrt{2E_{\rm TF}} = \left(\frac{3}{2}g\right)^{1/3}.$$

The energy in the Thomas-Fermi approximation is obtained from the normalization condition (152) giving

$$E_{\rm TF}(g) = \frac{1}{2}\left(\frac{3}{2}g\right)^{2/3}. \tag{162}$$

The Thomas-Fermi approximation is assumed to be valid for large $g\to\infty$. However, even then the wave function (161) is correct only for $x \ll x_0$, where it has an expansion

$$\psi_{\rm TF}(x) \simeq c_0 + c_2 x^2 + c_4 x^4,$$

with the coefficients

$$c_0 = \frac{x_0}{\sqrt{2g}}, \quad c_2 = -\frac{c_0}{2x_0^2}, \quad c_4 = -\frac{c_0}{8x_0^4}.$$

The behavior of the function (161) near the boundary $x = x_0$ is not correct. Also, this function is not appropriate to evaluate the mean kinetic energy, producing a divergence for any $g$ (see discussion in [73,75]). In order to understand when the total energy (162) for the Thomas-Fermi approximation starts giving reasonable results, we present in Fig. 5 the energies (158), (160), and (162). The first two energies, $E^*(g)$ and $E_2^*(g)$, almost coincide with each other, having correct asymptotic behavior in the weak- as well as in the strong-coupling limits. The Thomas-Fermi energy $E_{\rm TF}(g)$ possesses an incorrect weak-coupling limit and becomes a reasonable approximation starting from $g=7$.

The density

$$n(x) = |\psi(x)|^2 \tag{163}$$

for the corresponding wave functions and $g=0.2$ is presented in Fig. 6, where the density $n^*(x)=|\psi^*(x)|^2$ of the self-similar approximation (155) practically coincides with the density $n_G(x)=|\psi_G(x)|^2$ of the Gaussian approximation (159), as it should be in the weak-coupling limit. In this limit, the behavior of the density $n_{\rm TF}(x)=|\psi_{\rm TF}(x)|^2$ of the Thomas-Fermi approximation is not correct. As is known [73,75], the latter approximation is incorrect near the boundary even in the strong-coupling case. Then the density $n(x)$ in the self-similar approximation is close, except near the boundary, to that of the Thomas-Fermi approximation. The self-similar approximation $n^*(x)$ coincides with $n_{\rm TF}(x)$ for small $x$ and smoothes the incorrect behavior of $n_{\rm TF}(x)$ around the boundary. In the strong-coupling limit, the density $n_G(x)$ of the Gaussian approximation is not accurate.

The direct evaluation of the accuracy of each approximation can be done by calculating the residual term

$$R(x) \equiv H\psi(x) - (\psi, H\psi) \tag{164}$$

for Eq. (151), where $H$ is defined in Eq. (126) and $\psi(x)$ is a wave function of the corresponding approximation. The residual term for $g\gg 1$ for the self-similar approximation (155) is practically zero, meaning that Eq. (155) is an almost exact solution of Eq. (151). For the Gaussian approximation (159), the residual term is much larger, telling that this approximation is much less accurate. And the residual for the Thomas-Fermi approximation is divergent at the boundary point $x_0$, though far from this point it is close to zero.

The integral characteristic of accuracy of the corresponding solutions is the dispersion

$$\sigma(\psi) \equiv \left[\int_{-\infty}^{+\infty} |R(x)|^2 dx\right]^{1/2}. \tag{165}$$

We calculated this quantity for $0\leqslant g\leqslant 100$. The maximal dispersion for the self-similar approximation (155) is around 1, for the Gaussian approximation (159) it is about 20, and for the Thomas-Fermi approximation it is divergent.

In this way, the self-similar wave function (155) is the most accurate solution of the nonlinear Schrödinger equation (151), as compared to the Gaussian and Thomas-Fermi approximations. This function (155) represents the exact solution very well for all $x$ and $g$. In the weak-coupling limit $g$

$\rightarrow 0$, it becomes close to the Gaussian form, and in the strong-coupling limit, it approaches the Thomas-Fermi wave function for all $x$ except the boundary where it smoothes the incorrect behavior of the latter function. The crossover point between the weak-coupling and strong-coupling regimes occurs, as numerical calculations show, at around $g \approx 5$. This crossover point can also be evaluated, by an order of magnitude, analytically as follows. Notice that the characteristic length for the Gaussian function (159) is $x_G = \sqrt{2/u}$ with $u \approx 1$, and that such a length for the Thomas-Fermi function (161) is $x_0 = (3g/2)^{1/3}$. These characteristic lengths, typical of the weak-coupling and strong-coupling regimes, respectively, coincide, that is, $x_G = x_0$, at $g \approx 2^{5/2}/3 \approx 2$.

### B. Vortex filament equation

Now we shall show that our approach permits us to find accurate analytical approximations for the function describing the structure of vortex filaments. Considering an unbounded Bose system and making in the nonlinear Schrödinger equation the substitution $\psi(\vec{r}) = f(r)e^{i\varphi}$, in which $r$ and $\varphi$ are dimensionless polar coordinates, one comes [70,72] to the equation

$$\frac{d^2 f}{dr^2} + \frac{1}{r}\frac{df}{dr} - \frac{f}{r^2} + f - f^3 = 0. \tag{166}$$

The solution to this equation is usually obtained numerically [70,76,77]. Here we shall construct a sequence of analytical approximations for the solution to Eq. (166) and compare them with the known numerical data. Note that the equations similar to Eq. (166) have been considered as well for describing magnetic solitons [78], isomeric states of quantum fields [79], and vortices of complex scalar fields [80]. Therefore the possibility of deriving accurate analytical solutions to these equations is important for many applications, such as condensed Bose gas, superfluid helium, magnets in strong magnetic fields, and different models of quantum fields.

At small $r \rightarrow 0$, the solution to Eq. (166) has the asymptotic expansion

$$f(r) \simeq cr\left(1 - \frac{1}{8}r^2\right), \tag{167}$$

where $c$ is a constant. At large $r \rightarrow \infty$, one gets

$$f(r) \simeq 1 - \frac{1}{2}r^{-2} - \frac{9}{8}r^{-4} - \frac{169}{16}r^{-6}. \tag{168}$$

Employing the approach of Sec. II, we easily obtain the following sequence of self-similar approximants:

$$f_2^*(r,0) = c_2 r\left(1 + \frac{1}{4}r^2\right)^{-1/2},$$

$$f_3^*(r,0) = c_3 r\left(1 + \frac{1}{2}r^2 + \frac{1}{4}r^4\right)^{-1/4},$$

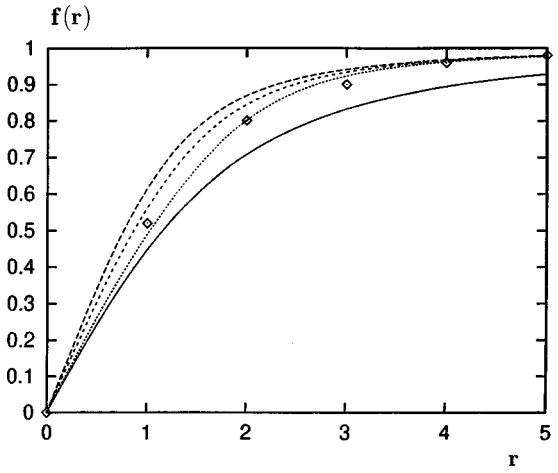


FIG. 7. The self-similar approximants $f_k^*(r,0)$, defined in Eq. (169), describing the structure of a vortex filament. The solid line is for $f_2^*(r,0)$, long-dashed line is for $f_3^*(r,0)$, short-dashed line is for $f_4^*(r,0)$, and the dotted line is for $f_5^*(r,0)$. Diamonds represent exact numerical data.

$$f_4^*(r,0) = c_4 r\left(1 + \frac{3}{4}r^2 + \frac{3}{16}r^4 + \frac{1}{16}r^6\right)^{-1/6},$$

$$f_5^*(r,0) = c_5 r\left(1 + r^2 + \frac{9}{70}r^4 + \frac{1}{35}r^6 + \frac{1}{140}r^8\right)^{-1/8}, \tag{169}$$

in which the coefficients, defined so as to give the correct asymptotic expansions, are

$$c_2 = 4^{-1/2} = 0.5, \quad c_3 = 4^{-1/4} = 0.707,$$

$$c_4 = 16^{-1/6} = 0.630, \quad c_5 = 140^{-1/8} = 0.539. \tag{170}$$

The behavior of the approximants $f_k^*(r,0)$ is shown in Fig. 7, compared with numerical data [70,76,77]. As can be concluded from this figure, $f_5^*(r,0)$ is a very accurate solution.

## VII. CONCLUSION

We have developed an approach for obtaining analytical solutions of quantum-mechanical problems. This approach makes it possible, starting from asymptotic expansions having sense only in the vicinity of limiting points, to derive interpolation formulas valid in the whole range of variables. The developed method is rather general and can be applied to various problems. We demonstrated its applicability to several quantum-mechanical models, such as different anharmonic oscillators, double-well potentials, resonance models with quasistationary states, and nonlinear Hamiltonians. The method permits one to construct accurate analytical expressions for energy levels as well as for wave functions. It is important that this method provides a regular procedure for deriving a convergent sequence of subsequent approximations, so that it is possible to reach the desired accuracy by calculating higher-order approximations. The idea of the approach is based on the self-similar approximation theory [8–17]]; this is why we call the method developed in the present

paper the self-similar interpolation. The method can find numerous practical applications, for example, for analyzing spectral properties of atoms and molecules, for studying the physics of quantum dots, and for investigating the behavior of Bose-condensed gases in magnetic traps.

**ACKNOWLEDGMENTS**

We appreciate financial support from the National Science and Technology Development Council of Brazil, and from the University of Western Ontario, Canada.

[1] G. A. Baker, Jr., G. S. Rushbrooke, and H. E. Gilbert, Phys. Rev. **135**, A1272 (1964).
[2] G. A. Baker, Jr. and J. D. Johnson, Phys. Rev. A **44**, 2271 (1991).
[3] G. A. Baker, Jr. and P. Graves-Morris, *Padé Approximants* (Cambridge University, Cambridge, England, 1996).
[4] O. V. Selyugin and M. A. Smondyrev, Phys. Status Solidi B **155**, 155 (1989).
[5] J. Čižek, E. J. Weniger, P. Bracken, and V. Špirko, Phys. Rev. E **53**, 2925 (1996).
[6] I. D. Feranchuk, L. I. Komarov, I. V. Nichipor, and A. P. Ulyanenkov, Ann. Phys. (N.Y.) **238**, 370 (1995).
[7] A. Okopińska, Ann. Phys. (N.Y.) **249**, 367 (1996).
[8] V. I. Yukalov, Phys. Rev. A **42**, 3324 (1990).
[9] V. I. Yukalov, Physica A **167**, 833 (1990).
[10] V. I. Yukalov, J. Math. Phys. **32**, 1235 (1991).
[11] V. I. Yukalov, J. Math. Phys. **33**, 3994 (1992).
[12] V. I. Yukalov and E. P. Yukalova, Physica A **206**, 553 (1994).
[13] V. I. Yukalov and E. P. Yukalova, Phys. Lett. A **225**, 336 (1996).
[14] V. I. Yukalov and S. Gluzman, Phys. Rev. Lett. **79**, 333 (1997).
[15] S. Gluzman and V. I. Yukalov, Phys. Rev. E **55**, 3983 (1997).
[16] V. I. Yukalov and S. Gluzman, Phys. Rev. E **55**, 6552 (1997).
[17] V. I. Yukalov, Mosc. Univ. Phys. Bull. **31**, 10 (1976).
[18] C. M. Bender and T. T. Wu, Phys. Rev. **184**, 1231 (1969).
[19] C. M. Bender and T. T. Wu, Phys. Rev. D **7**, 1620 (1973).
[20] B. Simon, Ann. Phys. (N.Y.) **58**, 76 (1970).
[21] F. T. Hioe and E. W. Montroll, J. Math. Phys. **16**, 1945 (1975).
[22] E. J. Weniger, Phys. Rev. Lett. **77**, 2859 (1996).
[23] J. Zinn-Justin, Phys. Rep. **70**, 109 (1981).
[24] B. Simon, Bull. Am. Math. Soc. **24**, 303 (1991).
[25] S. Graffi and V. Grecchi, J. Math. Phys. **19**, 1002 (1978).
[26] W. E. Caswell, Ann. Phys. (N.Y.) **123**, 153 (1979).
[27] I. Halliday and P. Suranyi, Phys. Rev. D **21**, 1529 (1980).
[28] P. M. Stevenson, Phys. Rev. D **23**, 2916 (1981).
[29] J. Killingbeck, J. Phys. A **14**, 1005 (1981).
[30] E. P. Yukalova and V. I. Yukalov, Phys. Lett. A **175**, 27 (1993).
[31] V. I. Yukalov and E. P. Yukalova, Laser Phys. **5**, 154 (1995).
[32] F. A. Buot, Phys. Rep. **234**, 73 (1993).
[33] S. Datta, *Electronic Transport in Mesoscopic Systems* (Cambridge University, Cambridge, England, 1995).
[34] U. Woggen, *Optical Properties of Semiconductor Quantum Dots* (Springer, Berlin, 1997).
[35] R. K. Pathak and K. Bhattacharyya, Int. J. Quantum Chem. **54**, 13 (1995).
[36] C. G. Callan, R. F. Dashen, and D. J. Gross, Phys. Rev. D **20**, 3279 (1979).
[37] J. B. Kogut, Phys. Rep. **67**, 67 (1980).
[38] R. Balsa, M. Plo, J. Esteve, and A. Pacheko, Phys. Rev. D **8**, 1945 (1983).
[39] R. Bishop, M. Flynn, M. Bosca, and R. Guardiola, Phys. Rev. A **40**, 6154 (1989).
[40] F. A. de Saavedra and E. Buendia, Phys. Rev. A **42**, 5073 (1990).
[41] S. B. Yuste and A. M. Sánchez, Phys. Rev. A **48**, 3478 (1993).
[42] A. V. Sergeev, J. Phys. A **28**, 4157 (1995).
[43] K. Bhattacharyya and R. K. Pathak, Int. J. Quantum Chem. **59**, 219 (1996).
[44] V. I. Yukalov and E. P. Yukalova, J. Phys. A **29**, 6429 (1996).
[45] K. Bhattacharyya and R. K. Pathak, J. Mol. Struct. **361**, 41 (1996).
[46] R. Karrlein and H. Kleinert, Phys. Lett. A **187**, 133 (1994).
[47] J. E. Drummond, J. Phys. A **15**, 2321 (1982).
[48] M. Consoli and P. M. Stevenson, Z. Phys. C **63**, 427 (1994).
[49] M. Consoli and P. M. Stevenson, Phys. Lett. B **391**, 144 (1997).
[50] A. Agodi, G. Andronico, P. Cea, M. Consoli, L. Cosmai, R. Fiore, and P. M. Stevenson, Mod. Phys. Lett. A **12**, 1011 (1997).
[51] R. Ibanez-Meier, I. Stancu, and P. M. Stevenson, Z. Phys. C **70**, 307 (1996).
[52] D. E. Pritchard, Phys. Rev. Lett. **51**, 1336 (1983).
[53] H. F. Hess, Phys. Rev. B **34**, 3476 (1986).
[54] W. Petrich, M. H. Anderson, J. R. Ensher, and E. A. Cornell, Phys. Rev. Lett. **74**, 3352 (1995).
[55] M. H. Anderson *et al.*, Science **269**, 198 (1995).
[56] K. B. Davis *et al.*, Phys. Rev. Lett. **75**, 3969 (1995).
[57] M. O. Mewes *et al.*, Phys. Rev. Lett. **77**, 416 (1996).
[58] H. W. Jackson, Phys. Rev. A **10**, 278 (1974).
[59] W. A. B. Evans, Nuovo Cimento B **30**, 145 (1975).
[60] M. Alexanian and R. A. Britto, Phys. Rev. B **17**, 3547 (1978).
[61] M. Alexanian, Physica A **100**, 45 (1980).
[62] P. Whitlock and R. Panoff, Can. J. Phys. **65**, 1409 (1982).
[63] G. C. Marques, Int. J. Mod. Phys. B **8**, 1577 (1994).
[64] K. Kirsten and D. J. Toms, Phys. Lett. A **222**, 148 (1996).
[65] K. Kirsten and D. J. Toms, Phys. Lett. B **368**, 119 (1996).
[66] K. Kirsten and D. J. Toms, J. Res. Natl. Inst. Stand. Technol. **101**, 47 (1996).
[67] H. Haugerud, T. Haugset, and F. Ravndal, Phys. Lett. A **225**, 18 (1997).
[68] F. Brosens, J. T. Devreese, and L. F. Lemmes Solid State Commun. **100**, 123 (1996).
[69] E. P. Gross, Phys. Rev. **106**, 161 (1957).
[70] V. L. Ginzburg and L. P. Pitaevskii, J. Exp. Theor. Phys. **7**, 858 (1958).
[71] L. P. Pitaevskii, J. Exp. Theor. Phys. **13**, 451 (1961).
[72] E. P. Gross, J. Math. Phys. **4**, 195 (1963).
[73] D. Dalfovo, L. Pitaevskii, and S. Stringari, J. Res. Natl. Inst. Stand. Technol. **101**, 537 (1996).

[74] R. J. Dodd, J. Res. Natl. Inst. Stand. Technol. **101**, 545 (1996).
[75] E. Lundh, C. J. Pethick, and H. Smith, Phys. Rev. A **55**, 2126 (1997).
[76] A. L. Fetter, in *Quantum Fluids and Nuclear Matter*, edited by K. T. Mahanthappa and W. E. Britten (Gordon and Breach, New York, 1969), p. 321.
[77] V. L. Ginzburg and A. A. Sobyanin, J. Exp. Theor. Phys. **55**, 455 (1982).
[78] A. M. Kosevich, B. A. Ivanov, and A. S. Kovalev, Phys. Rep. **194**, 117 (1990).
[79] A. M. Polyakov, J. Exp. Theor. Phys. **41**, 988 (1975).
[80] J. C. Neu, Physica D **43**, 385 (1990).